Massachusetts Institute of Technology
22.68J/2.64J
Superconducting Magnets

⇓

May 1, 2003

- Lecture #9 – AC Losses
  - AC Losses
  - Joint Losses

AC Loss Components

- Hysteresis: $P_h \propto \dot{B}_e$
  - Intrinsic to superconductor and because Type II, when exposed to B_e, is in mixed state.
  - Theory agrees reasonably well with experiment.
- Coupling: $P_c \propto \dot{B}_e^2$
  - Joule dissipation of a dB/dt-induced filament-to-filament (intra-strand) coupling current in the matrix metal.
  - Theory well-understood but exact computation not possible because some parameter values are not well known.
  - Inter-strand coupling between composite strands in a cable is particularly difficult to calculate.
- Eddy-current: $P_e \propto \dot{B}_e^2$
  - Joule dissipation of dB/dt-induced current in the resistive matrix metal not occupied by a cluster of filaments.
  - Theory, e.g. problem 2.7, useful.

Parameters Affecting AC Losses

- Critical Properties: J_c (B,T)
- Magnetic field:
  - Bias (DC); amplitude (AC); frequency, phase.
  - Orientation (transverse, parallel, rotating)
- Current:
  - Bias (DC); Amplitude (AC); frequency, phase.
- Composite Material Properties:
  - Resistivity; geometry.
- Multistrand Cables and Braids:
  - Configuration; twist pitches; contact resistances.

Implications for Superconductor Design

- Decrease Hysteresis Loss:
  - Reduce superconductor dimension
    - Many small superconducting filaments
- Decrease Coupling Loss:
  - Twist Wire $\rightarrow$ Twist filaments
  - Reduce twist pitch
    - Reduce wire size
  - Increase transverse resistivity
    - Add internal barriers
- Make Multistrand Cables and Braids:
  - For high current
  - Low AC losses

Relevant Superconducting Wires are Complex Composites

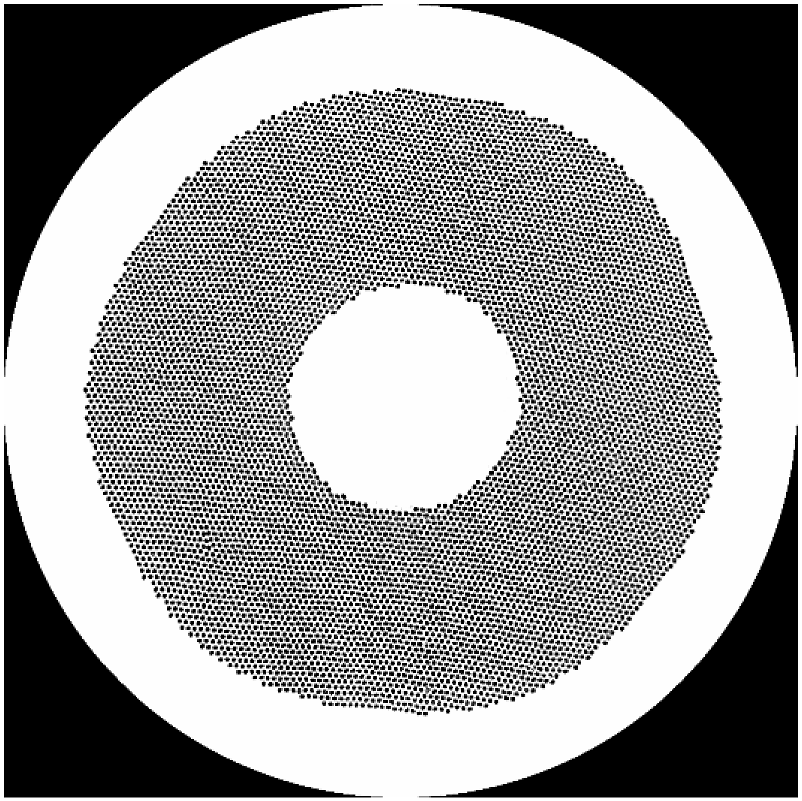

Typical SSC Nb-47wt.%Ti strand (OST manufacture).

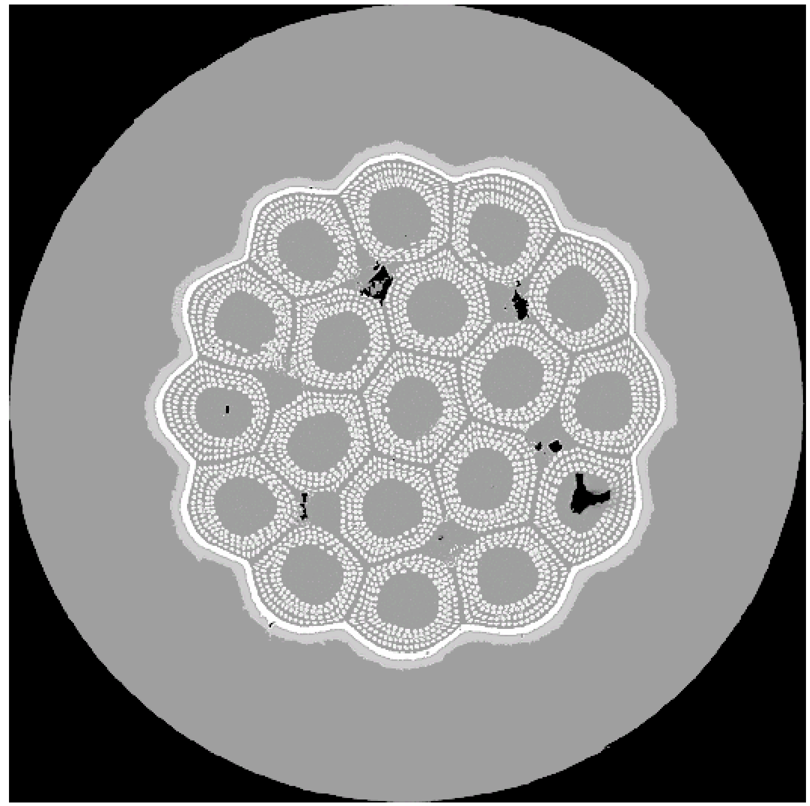

Typical reacted ITER Nb_3Sn strand (IGC manufacture).

Field Penetration in a Slab – Bean Model

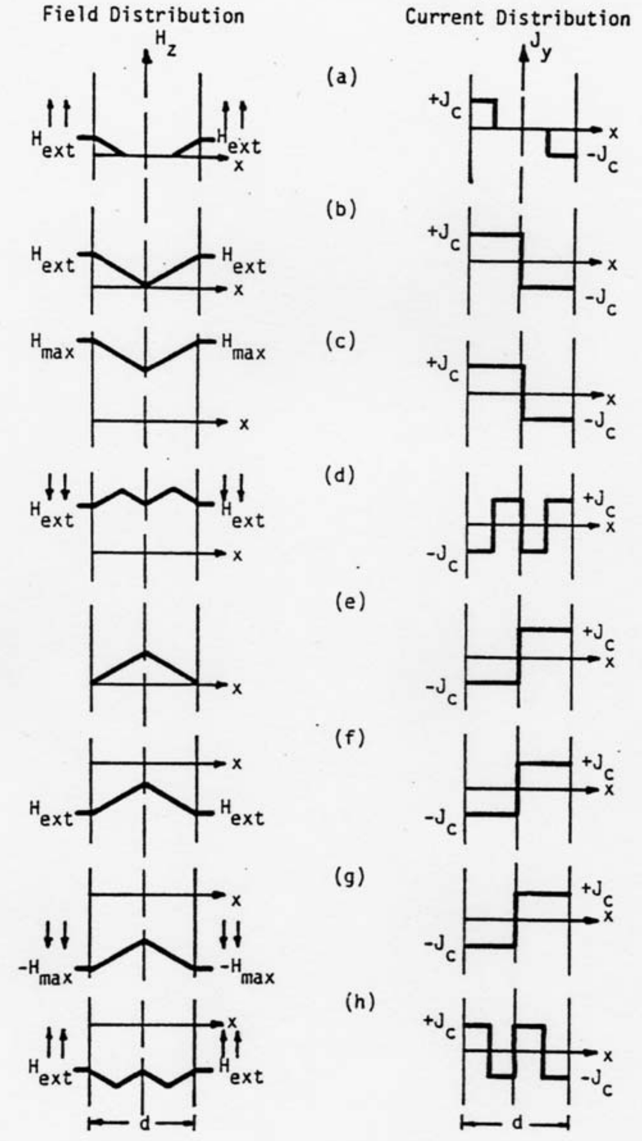

Fig. III.1. Field and current distribution in a type II superconducting slab of thickness d with external field applied parallel to the slab surfaces.

AC Loss Expressions

Hysteresis

Assumption: Bean-London model applies, i.e., $J_c \neq f(B)$

H_p – Field required to fully penetrate a slab:

$$H_p = \frac{J_c}{2} d$$

W_h/V -Loss per cycle per unit volume:

$$H_m \leq H_p$$

$$\frac{W_h}{V} = \frac{2}{3} \mu_o H_p^2 \left(\frac{H_m}{H_p} \right)^3$$

$$H_m \geq H_p$$

$$\frac{W_h}{V} = \frac{2}{3} \mu_o H_p^2 \left[3\left(\frac{H_m}{H_p} \right) - 2 \right]$$

Simplified AC Loss Expressions

Normalize to full-penetration field loss:

$$\frac{W_o}{V} = \frac{2}{3}\mu_o H_p^2$$

Then:

$$\frac{H_m}{H_p} \le 1,$$

$$\frac{W_h}{W_o} = \left(\frac{H_m}{H_p}\right)^3$$

$$\frac{H_m}{H_p} \ge 1,$$

$$\frac{W_h}{W_o} = \left[3\left(\frac{H_m}{H_p}\right) - 2\right]$$

And for: $\frac{H_m}{H_p} >> 1$, $\frac{W_h}{W_o} \approx 3\left(\frac{H_m}{H_p}\right)$

Field Penetration in a Slab – Kim Model

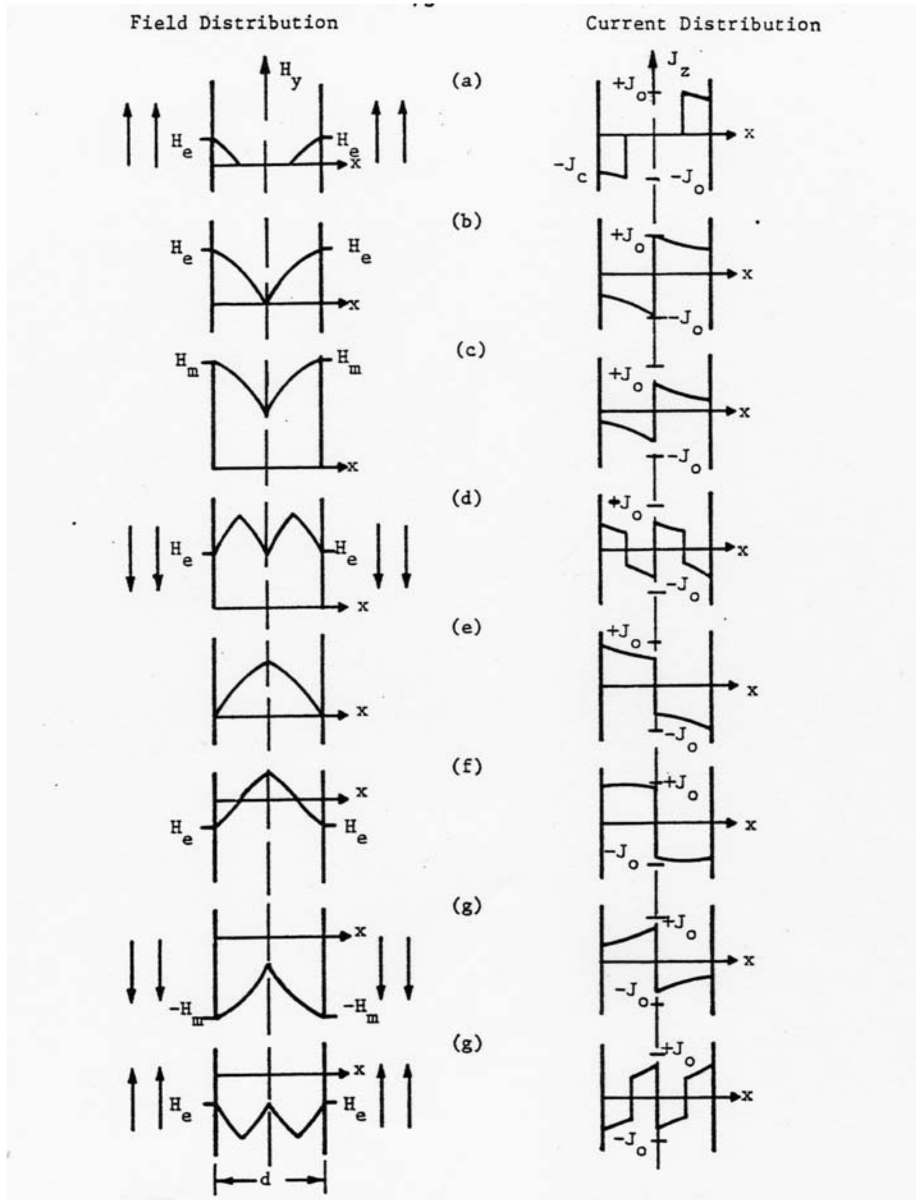

Fig. III.3. Kim model of field and current distributions in a Type II superconducting slab of thickness d with external field applied parallel to the surface.

Schematic for Magnetization Measurement Using Pick-Up Coils

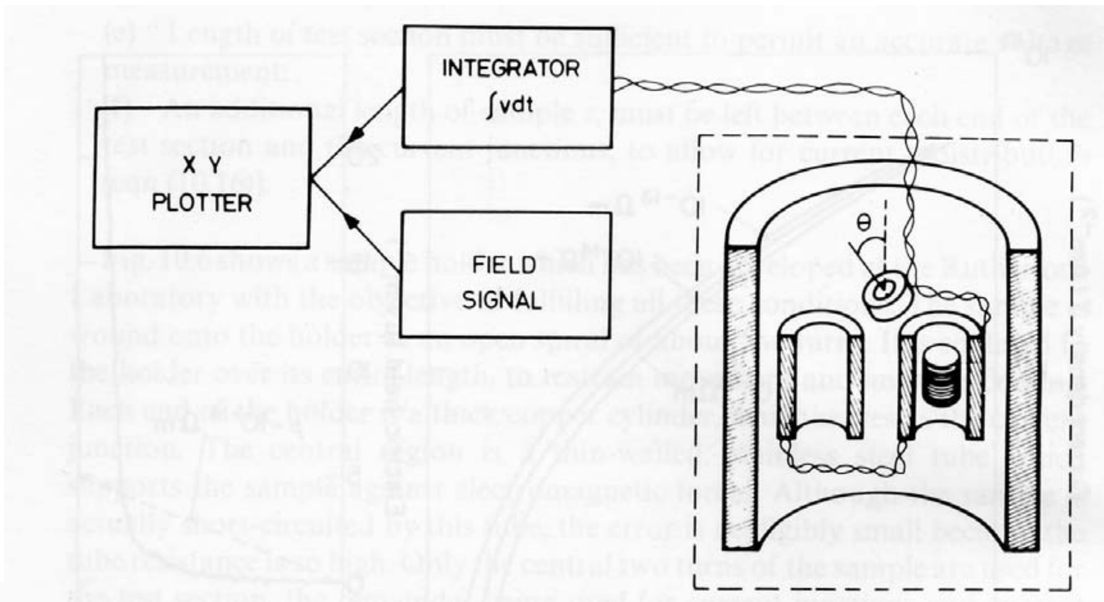

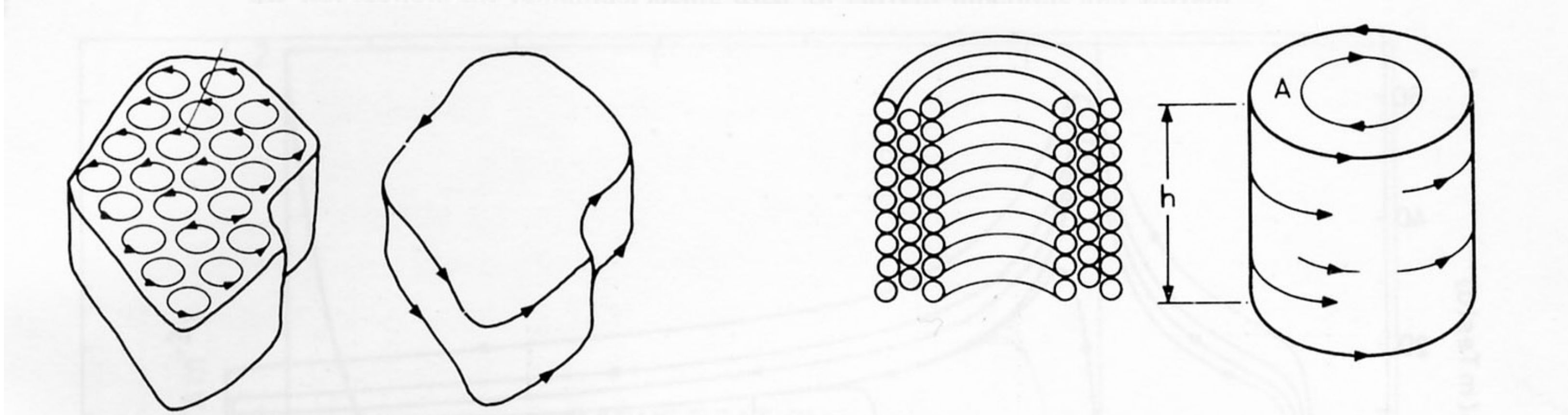

Technical Type II Superconductors Display a Magnetic Hysteresis

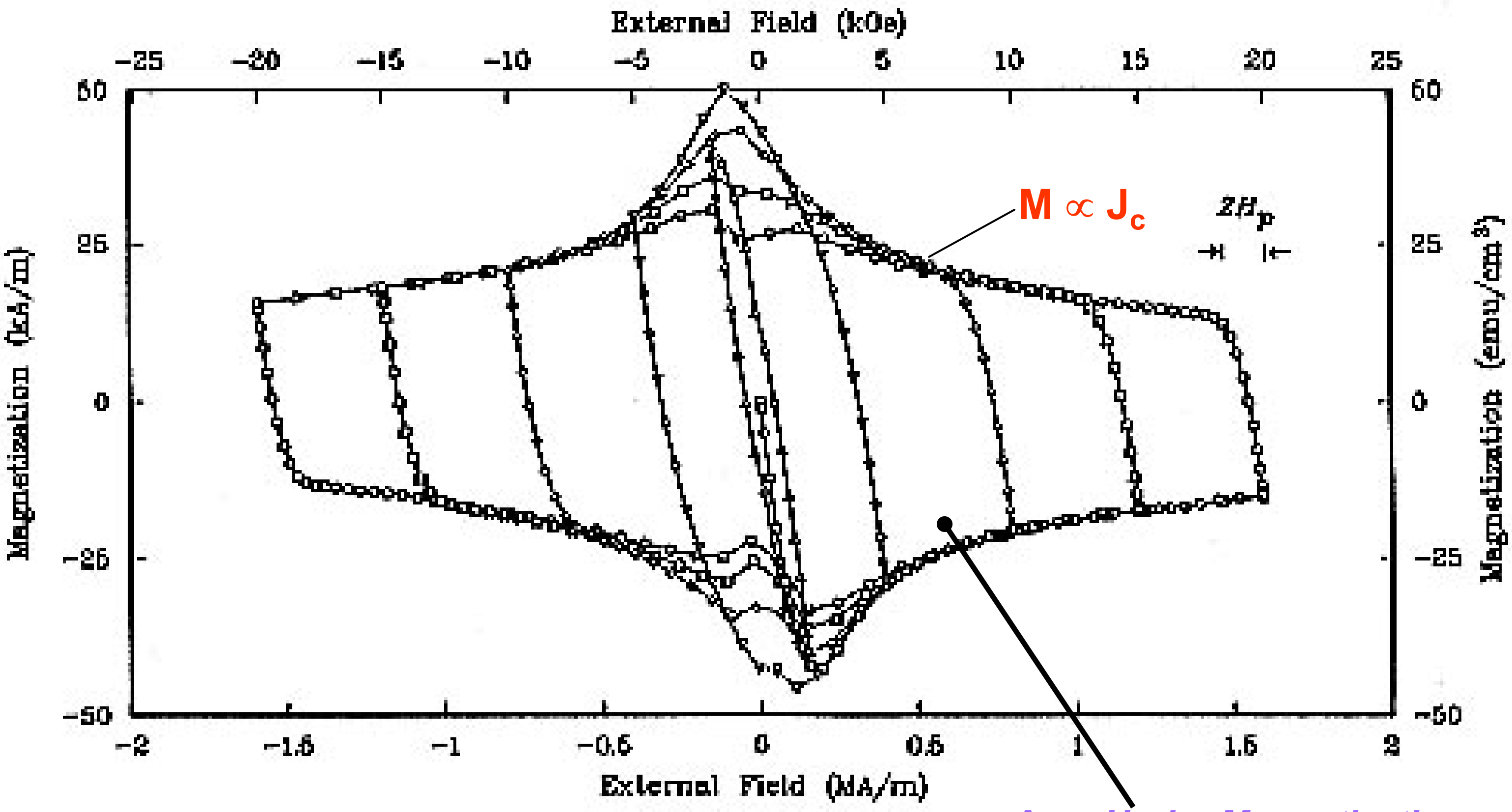

Area Under Magnetization Loop is Proportional to Dissipated Energy/cycle $\propto \Delta B\, J_c\, d_{eff}$

Calorimetric Measurement Method

- Measures vapor boiloff rate, $\dot{\mathcal{V}}$, at room temperature.

$$\dot{\mathcal{V}} = \frac{\varrho(T_b)}{\varrho(293\,\mathrm{K})} \times \frac{Q_{ac}}{h_L}$$

  ◇ LHe: $\dfrac{\varrho(T_b)}{\varrho(293\,\mathrm{K})h_L} = \dfrac{749}{(2.6\,\mathrm{J/cm^3})} = 288\,\mathrm{cm^3/J}$

  LN2: $\dfrac{\varrho(T_b)}{\varrho(293\,\mathrm{K})h_L} = \dfrac{690}{(161\,\mathrm{J/cm^3})} = 4.3\,\mathrm{cm^3/J}$

  ◇ Method generally applicable only to LHe — $4.3\,\mathrm{cm^3/J}$ (LN2) too small for accurate measurement.

- Important variables: pressure; liquid level; flow rate ($\dot{\mathcal{V}}$).

  ◇ Most important to keep $\dot{\mathcal{V}}$ constant.

Calorimetric Measurement Method

Constant-Flow Calorimeter (Takayasu, Gung, Minervini)

- $\dot{\mathcal{V}}$ kept constant by feed-back controlling Q_{heater} to keep the sum, $Q_{ac} + Q_{heater}$, constant.

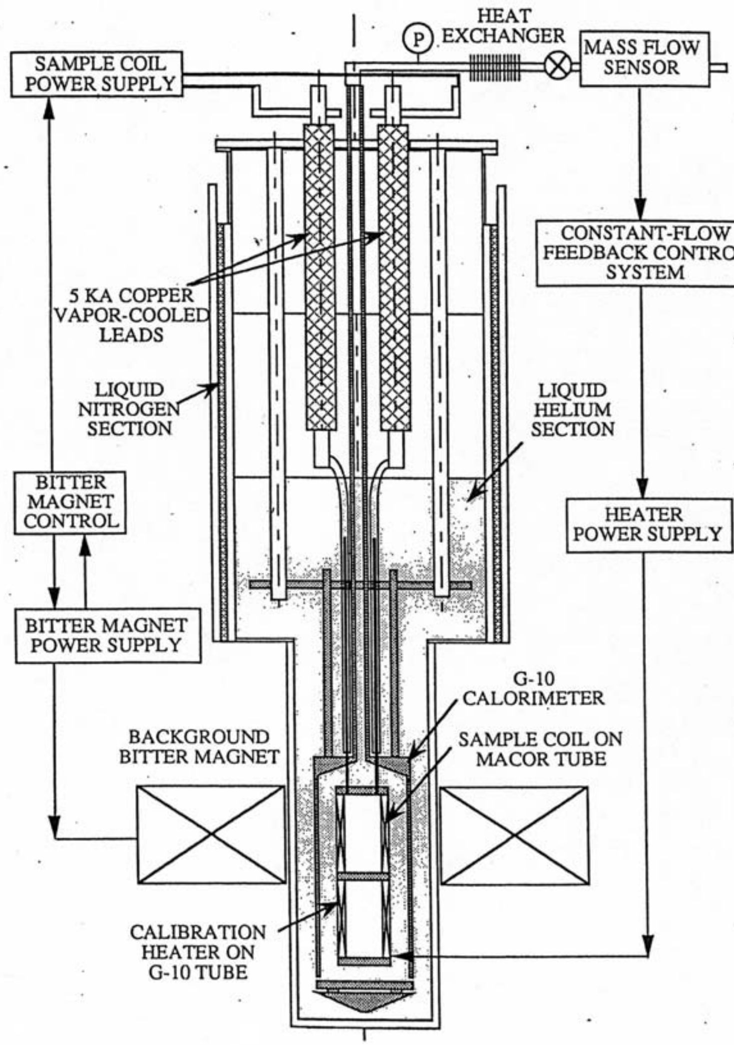

Field Penetration in a Slab – Bean Model with Transport Current

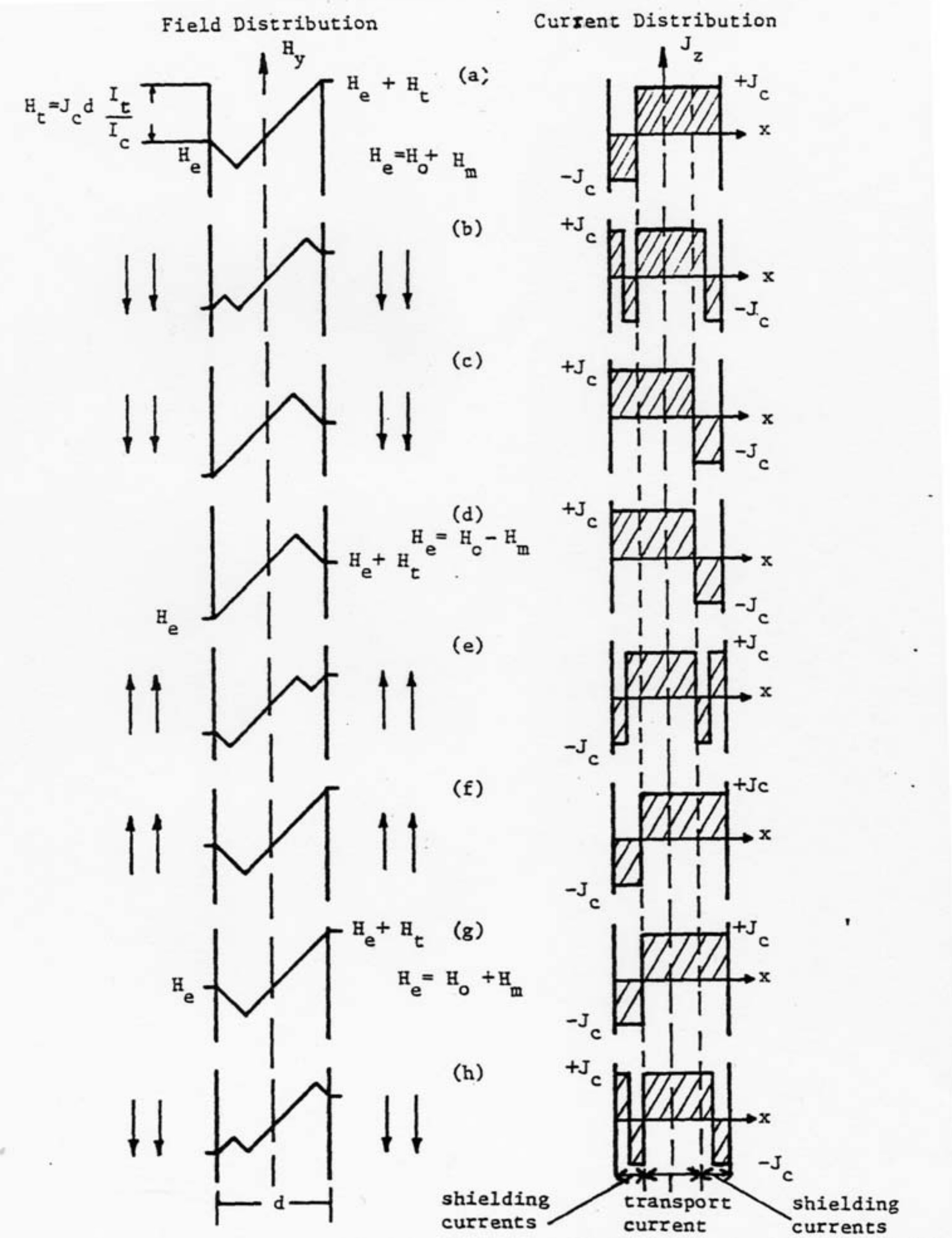

Fig. III.4. Bean model of field and current distribution in a slab carrying a transport current, $\frac{I_t}{I_c} = 0.5$

Effect of Transport Current

$$H_p(I) = \frac{J_c d}{2}\left(1 - \frac{I_t}{I_c}\right)$$

$$i = \frac{I_t}{I_c}$$

$$H_{po} = \frac{J_c d}{2}$$

$$H_p(i) = H_{po}(1 - i)$$

Transport current will increase the loss for the same magnetic field change if the $\Delta H > H_p(i)$.

Effect of Transport Current

$$\frac{W_o}{V} = \frac{2}{3}\mu_o H_p^2(0)$$

$$\frac{H_m}{H_p(i)} \leq 1,$$

$$\frac{W_h(i)}{W_o} = \left(\frac{H_m}{H_p(0)}\right)^3$$

$$\frac{H_m}{H_p(i)} \geq 1,$$

$$\frac{W_h(i)}{W_o} = \left(1 - i^3\right) + 3\left[\left(\frac{H_m}{H_p(0)}\right) - \left(\frac{H_p(i)}{H_p(0)}\right)\right]\left(1 + i^2\right)$$

Effect of Transport Current

$$\frac{H_m}{H_p(i)} \le 1 \quad \text{or} \quad \frac{H_m}{H_p(0)} \le (1-i),$$

$$\frac{W_h(i)}{W_o} = \frac{W_s(i)}{W_o} + \frac{W_t(i)}{W_o} = \left(\frac{H_m}{H_p(0)}\right)^3$$ **Total Loss**

Where

$$\frac{W_s(i)}{W_o} = \left(\frac{H_m}{H_p(0)}\right)^3$$ **Shielding Loss**

$$\frac{W_t(i)}{W_o} = 0$$ **Transport Loss**

Effect of Transport Current

$$\frac{H_m}{H_p(i)} \geq 1 \quad \text{or} \quad \frac{H_m}{H_p(0)} \geq (1-i),$$

$$\frac{W_h(i)}{W_o} = \frac{W_s(i)}{W_o} + \frac{W_t(i)}{W_o} = (1-i)^3 + 3\left[\left(\frac{H_m}{H_p(0)}\right) - \left(\frac{H_p(i)}{H_p(0)}\right)\right]\left(1+\mathrm{i}^2\right) \qquad \textbf{Total Loss}$$

Where

$$\frac{W_s(i)}{W_o} = (1-i)^3 + 3\left[\left(\frac{H_m}{H_p(0)}\right) - \left(\frac{H_p(i)}{H_p(0)}\right)\right]\left(1-\mathrm{i}^2\right) \qquad \textbf{Shielding Loss}$$

$$\frac{W_t(i)}{W_o} = 6\left[\left(\frac{H_m}{H_p(0)}\right) - \left(\frac{H_p(i)}{H_p(0)}\right)\right]\mathrm{i}^2 \qquad \textbf{Transport Loss}$$

Bean Model with Transport Current

Shielding Loss in a Slab

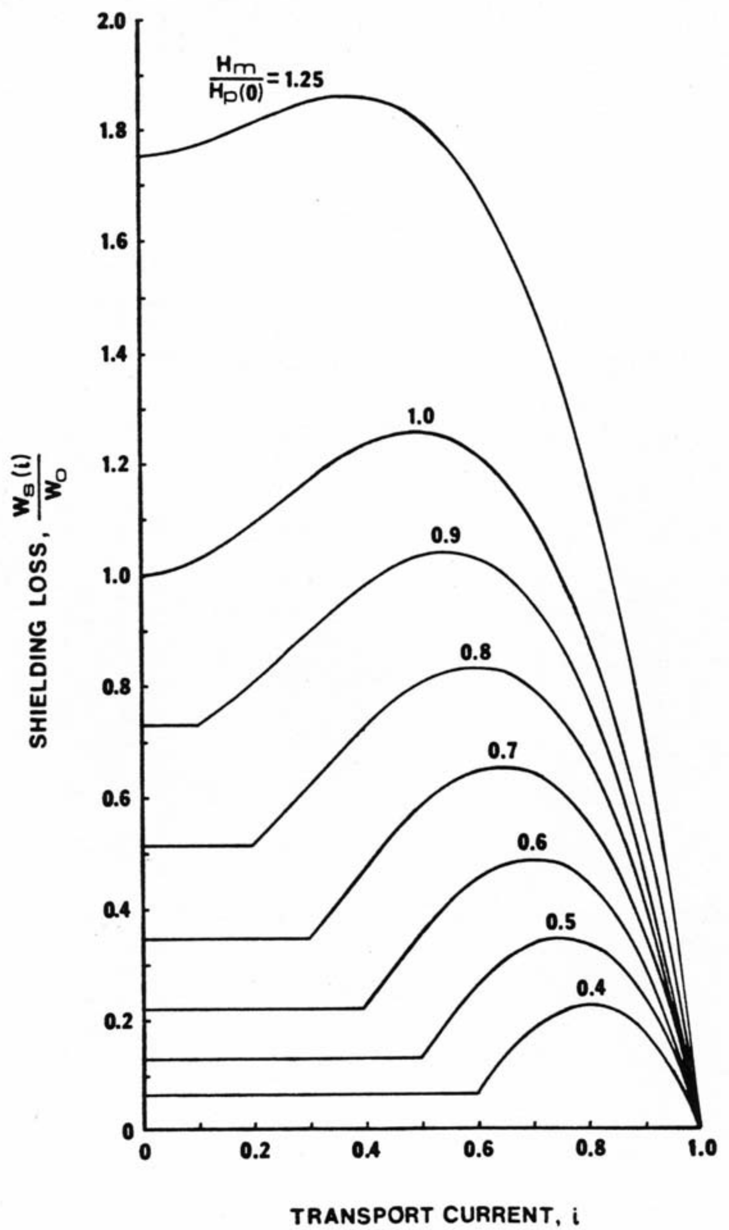

Figure 4.3-5. The shielding loss in a slab as a function of the transport current with maximum field change as a parameter.

Bean Model with Transport Current

Transport Loss in a Slab

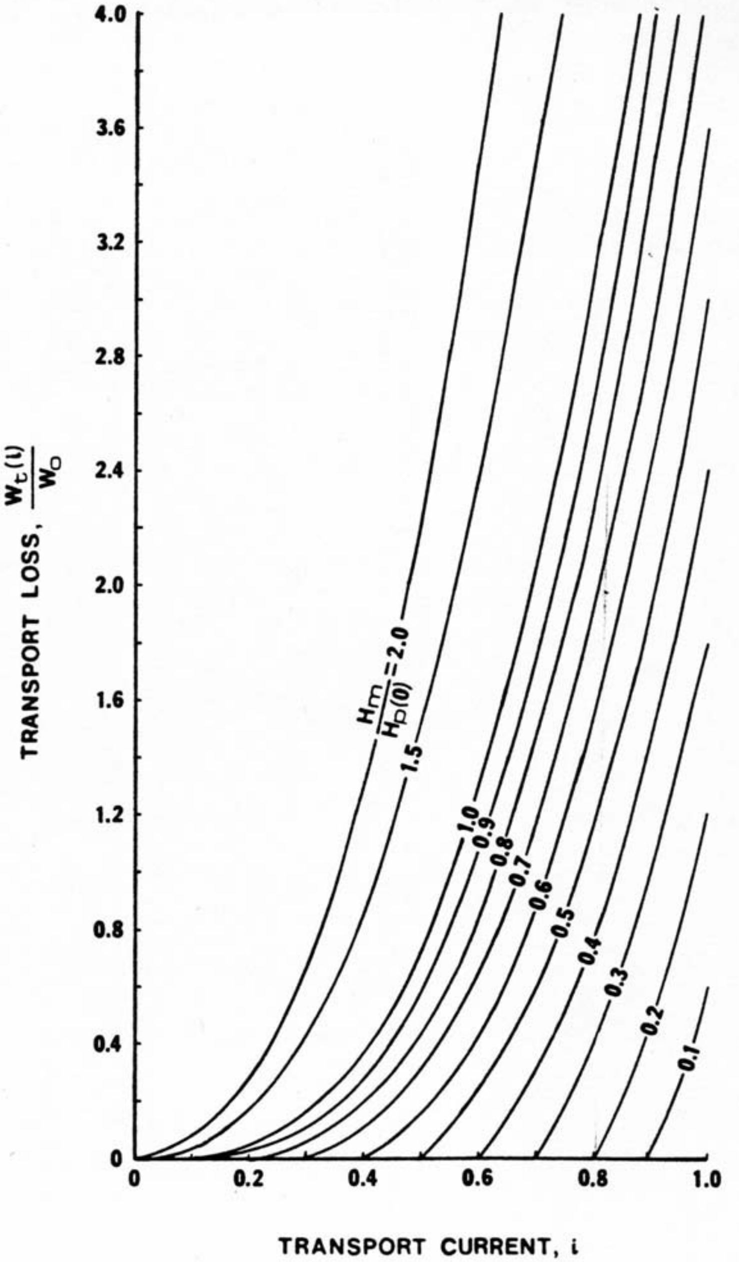

Figure 4.3-6. The transport loss in a slab as a function of transport current with maximum field change as a parameter.

Bean Model with Transport Current

Total Loss in a Slab vs Transport Current

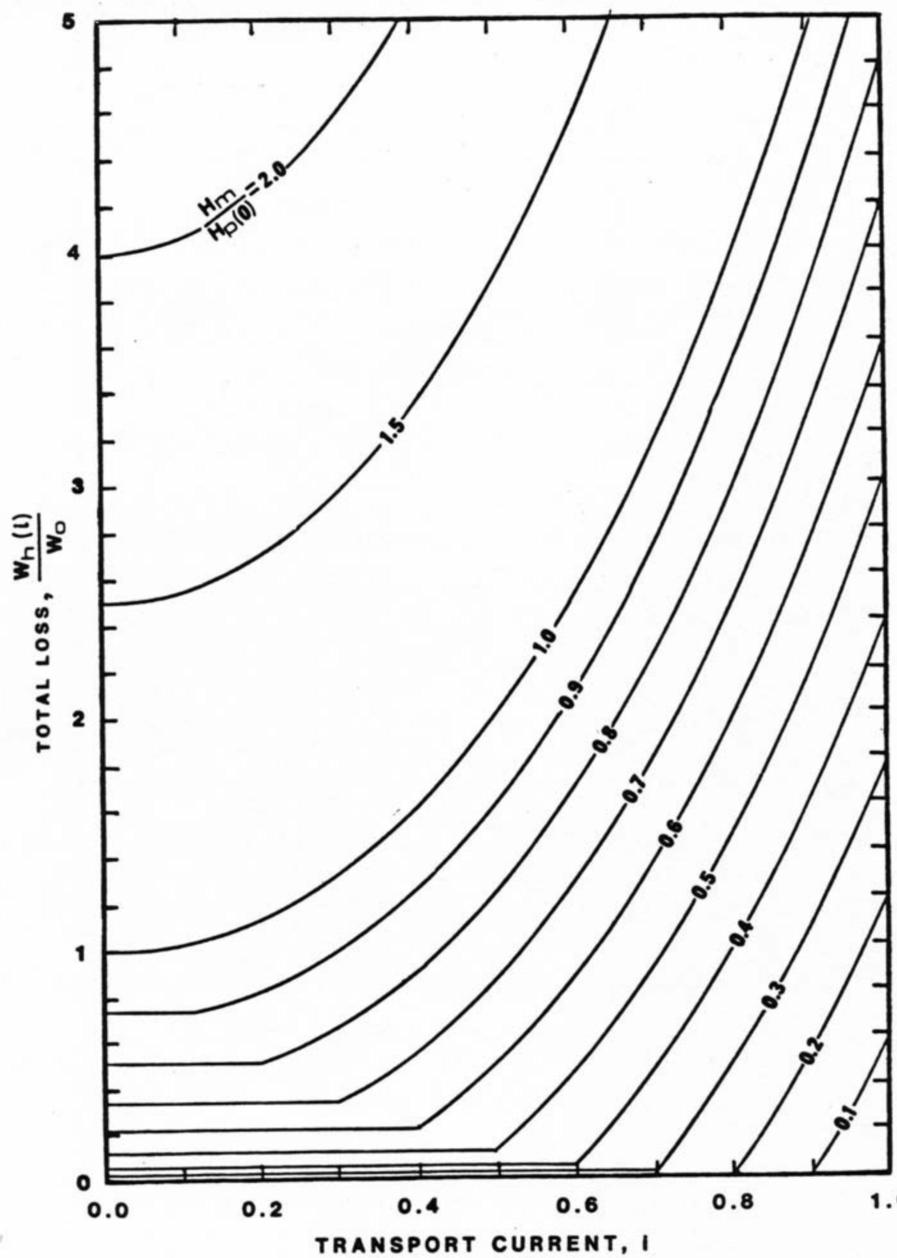

Figure 4.3-7. Total hysteresis loss in a slab as a function of transport current with maximum field change as a parameter. These data are the same as that in Figure 4.3-4.

Bean Model with AC Transport Current and Field in Synchronization

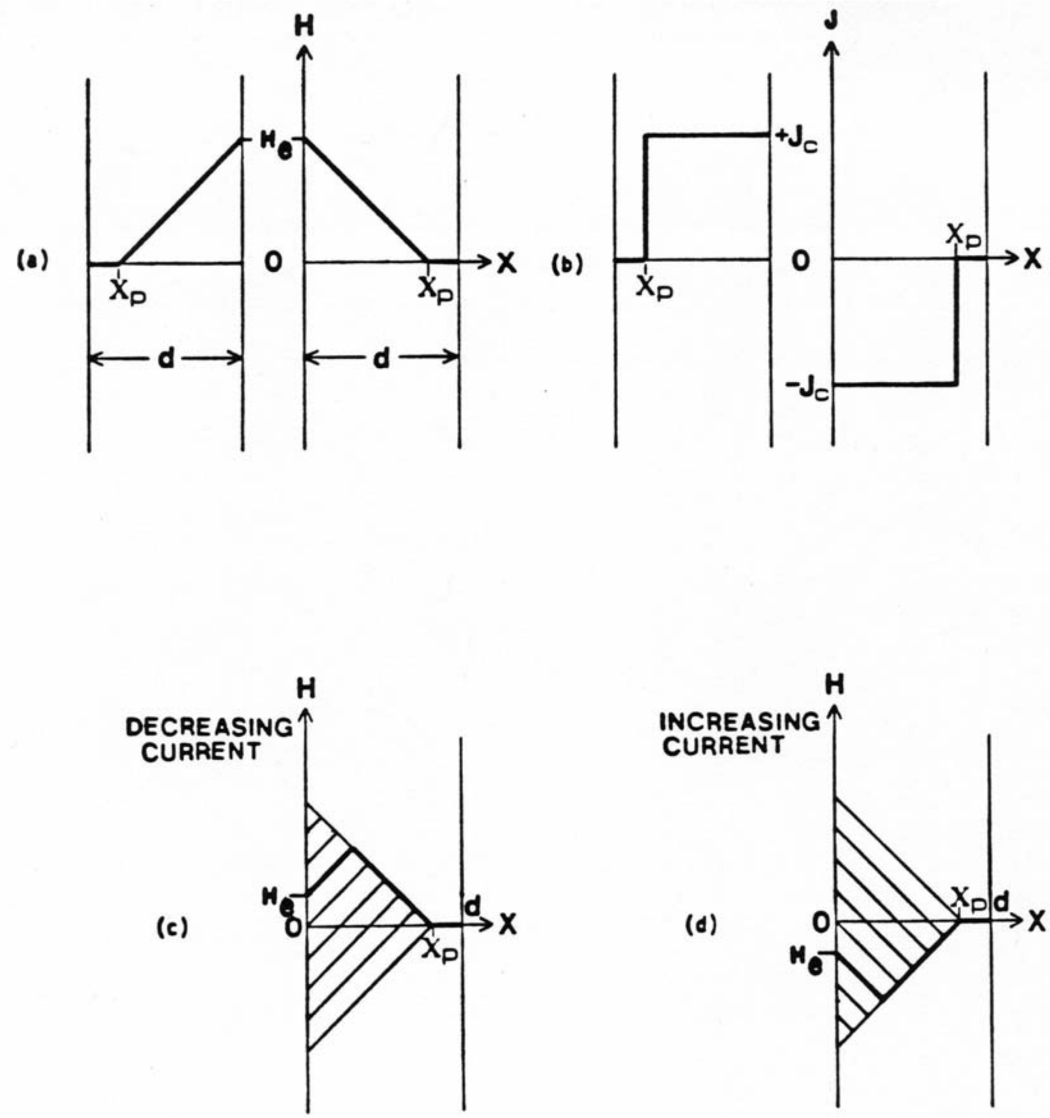

Figure 4.3-8. a) Field and b) current distributions in a slab carrying an alternating current in a constant background field; c) and d) are sequences of field profiles for decreasing and increasing current, respectively.

Bean Model with AC Transport Current

Terminal Voltage and Transport Current versus Time

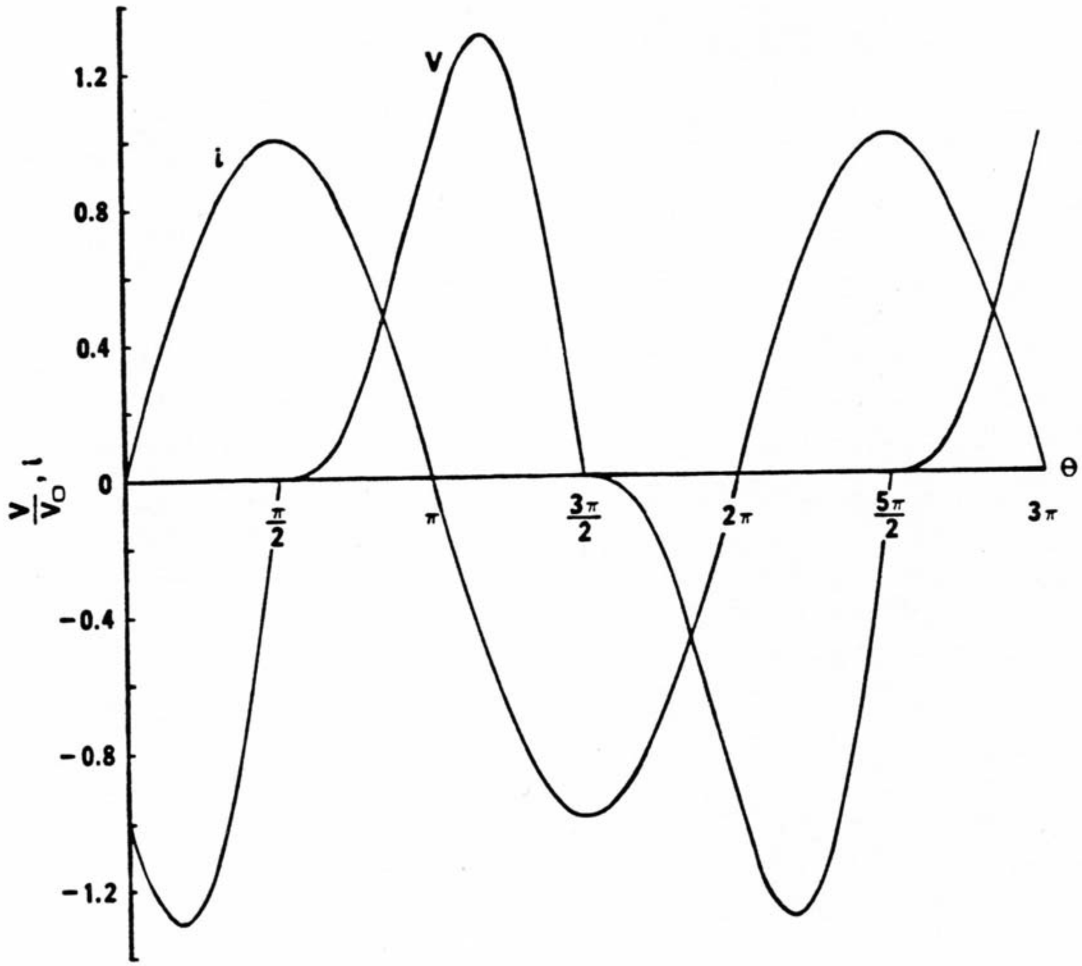

Figure 4.3-9. Terminal voltage, V, if a slab carrying an alternating current, i, in a constant background field as a function of time.

Bean Model with AC Transport Current

Terminal Voltage as a Function of Transport Current

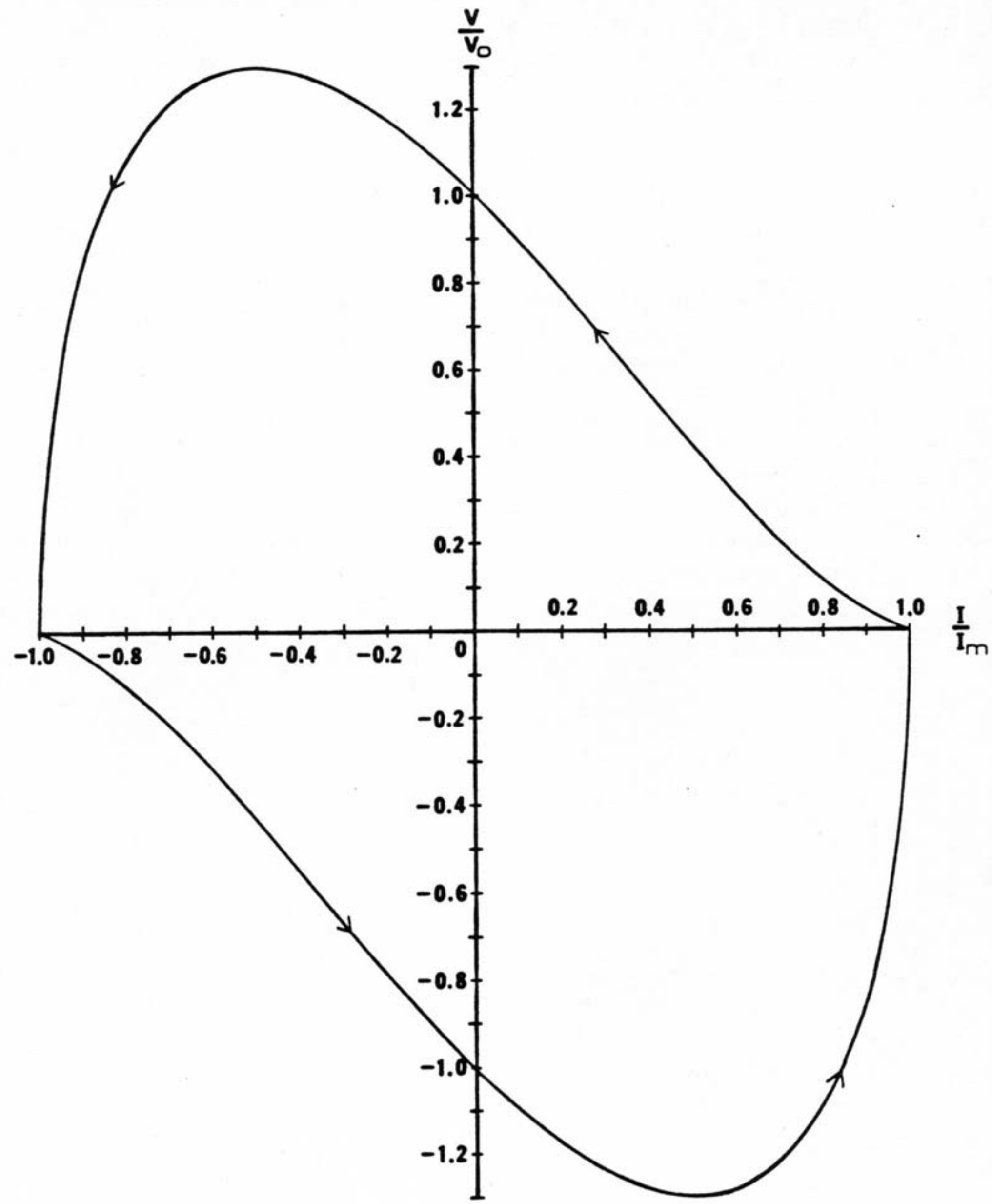

Figure 4.3-10. Terminal voltage of a slab as a function of the alternating transport current.

Bean Model

Circular Filament in a Transverse Field

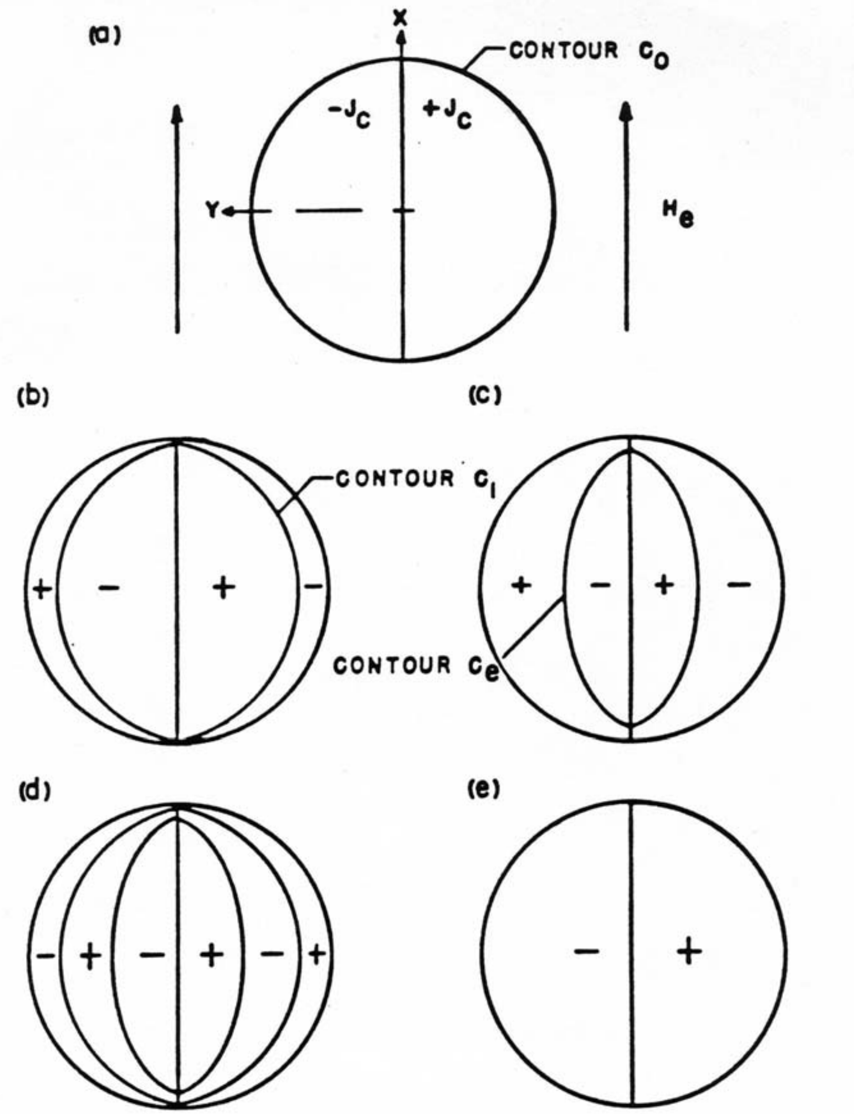

Figure 4.3-11. a) Initial condition at $H_0 + \Delta H_e$. b) Field reduced to $H_0 + \Delta H_e - \Delta H_1$. c) Lower limit of field change $H_0 - \Delta H_e$. d) Field increased to $H_0 - \Delta H_e + \Delta H_2$. e) End of half cycle with $H_0 + \Delta H_e$. Note: currents bounded by contour C shield $\Delta H/2$.

Transverse Flux Penetration into a Circular Superconducting Filament

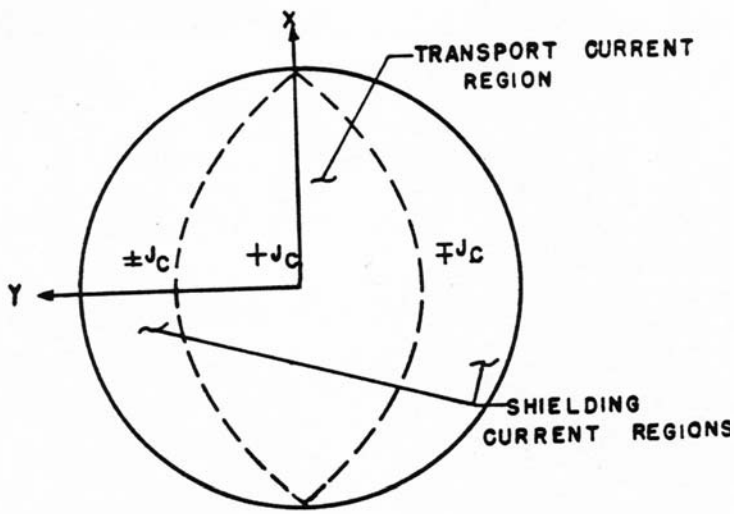

Figure 4.3-14. Current distribution in a circular filament showing the shielding current region and the transport current region.

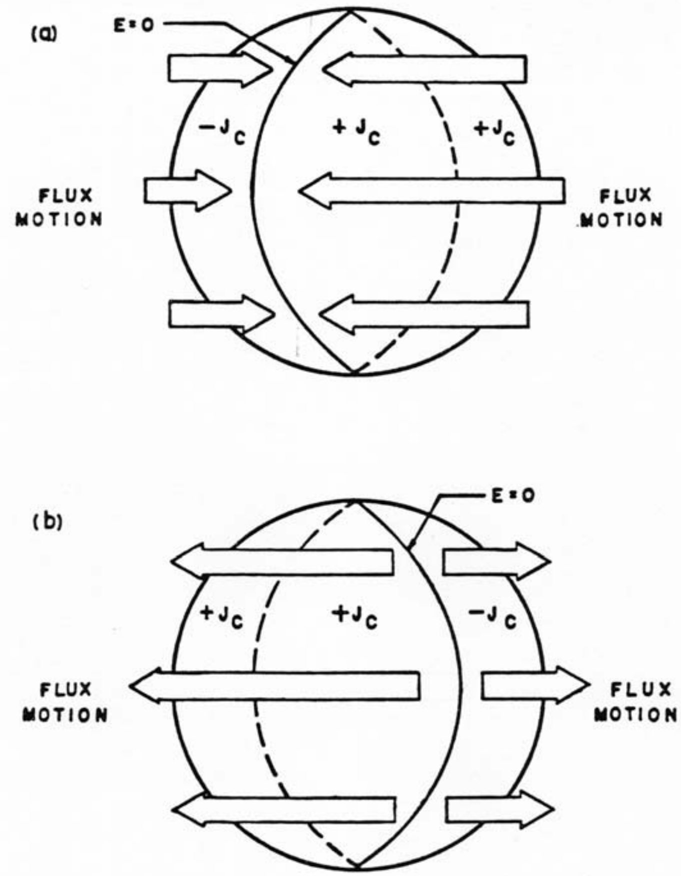

Figure 4.3-16. Full penetration flux motion for a) increasing external field, and b) decreasing external field.

Bean Model

Circular Filament in a Transverse Field

Numerical Solution

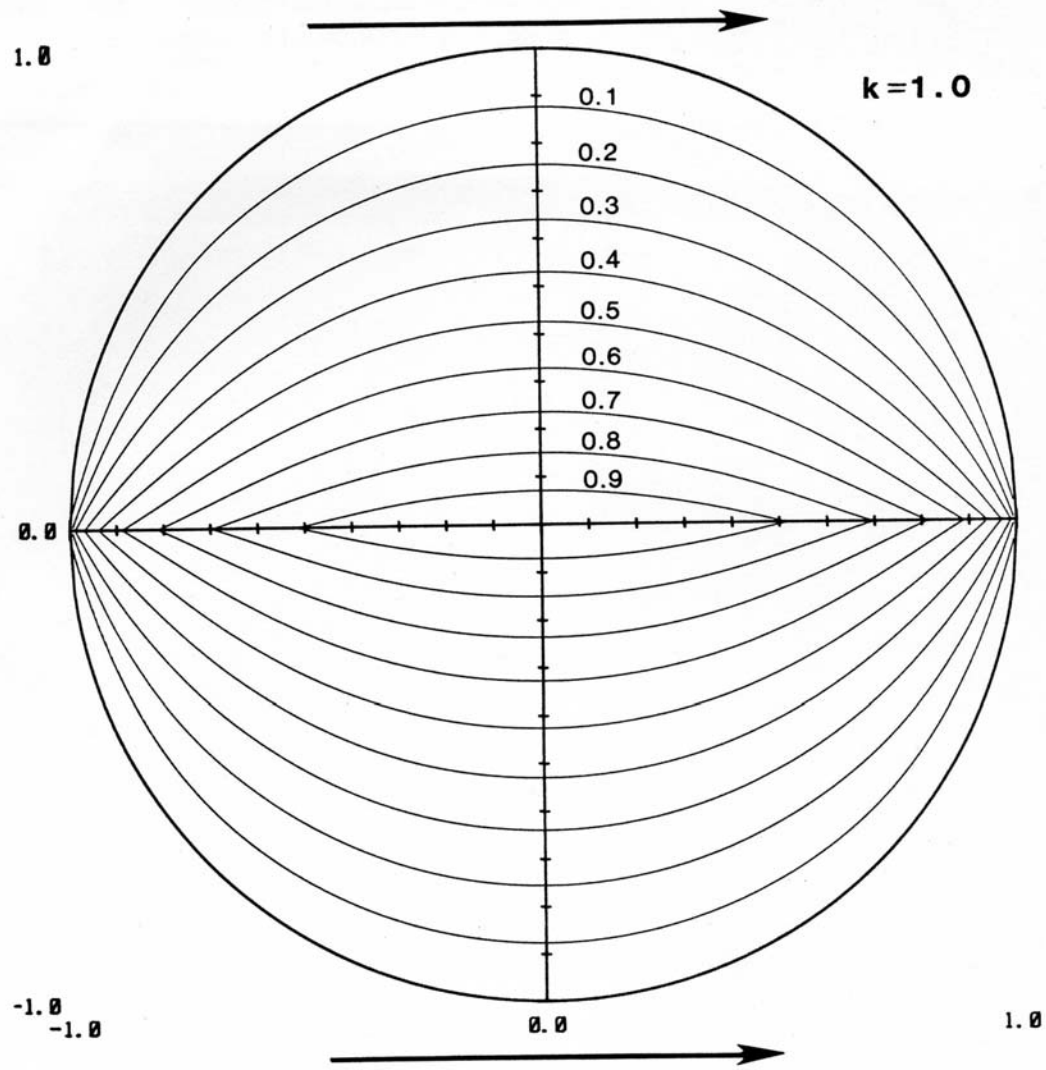

Figure 4.3-12. a) Limits of transverse flux penetration into cylindrical filaments of circular cross section for different values of the external field change $\Delta H_e/H_p(0)$.

Bean Model
Elliptical Filament in a Transverse Field
Numerical Solution

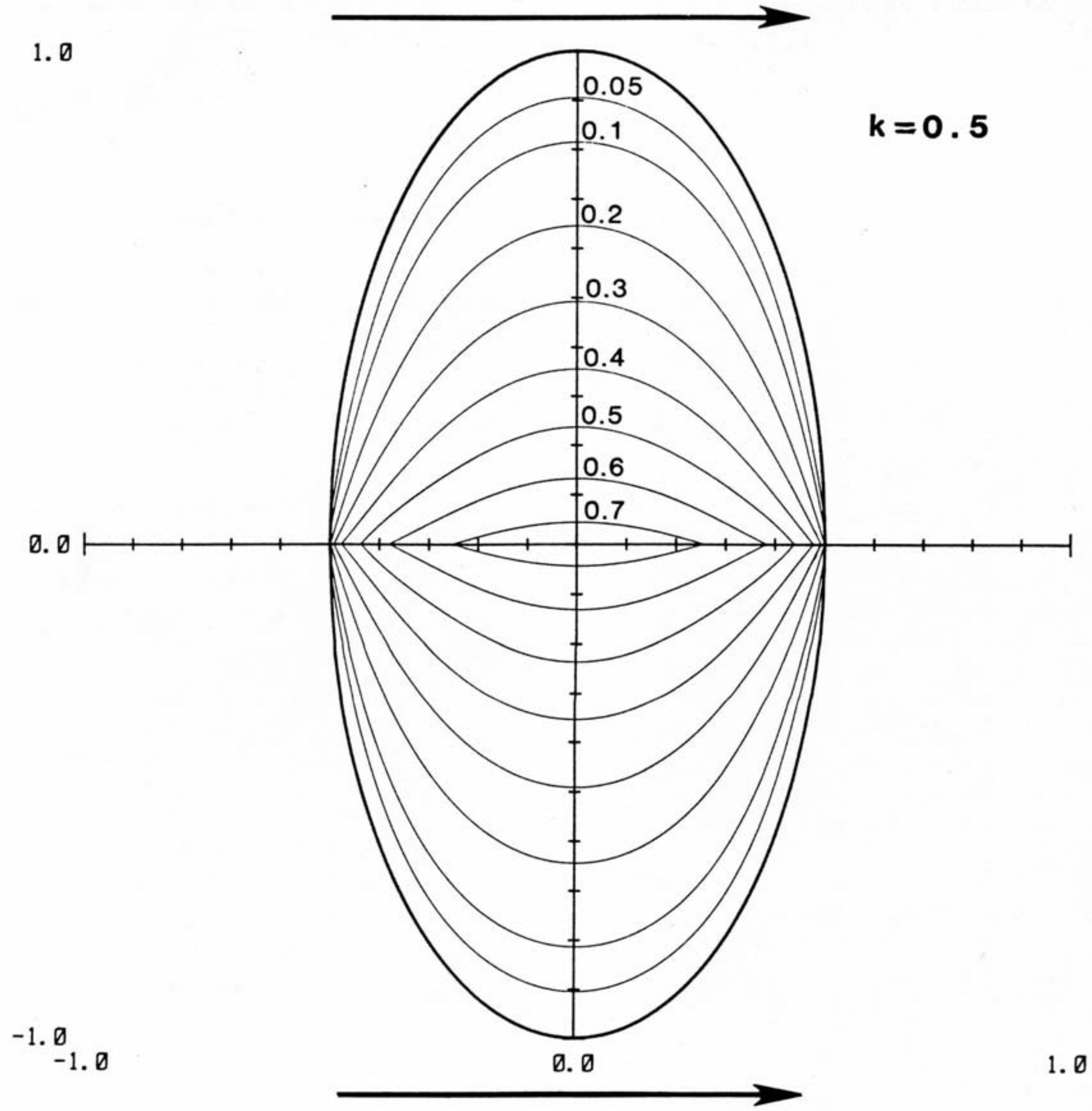

Figure 4.3-12 b) Limits of transverse flux penetration into cylindrical filaments of elliptical cross section for different values of the external field change $\Delta H_e/H_p(0)$ along the minor axis.

Bean Model
Elliptical Filament in a Transverse Field
Numerical Solution

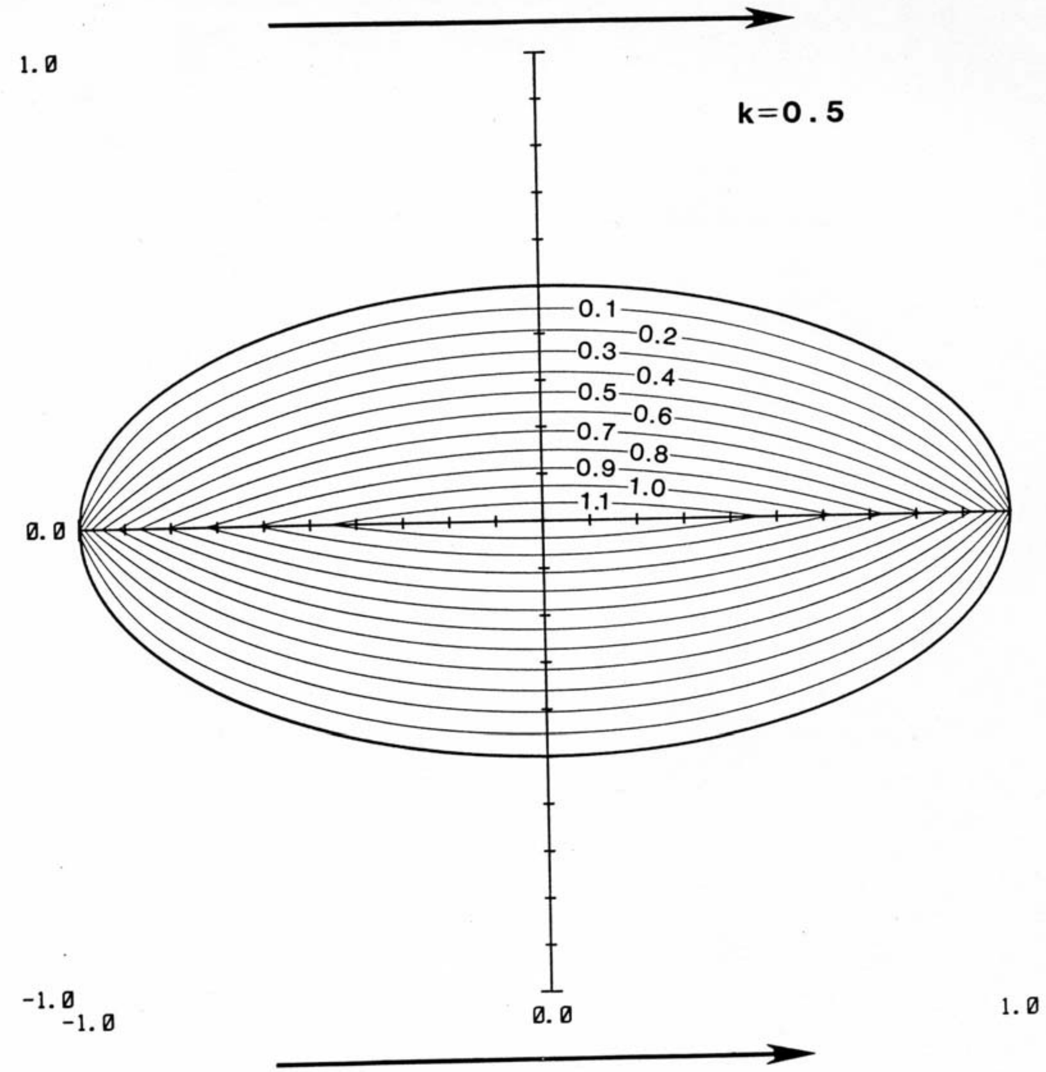

Figure 4.3-12 c) Limits of transverse flux penetration into cylindrical filaments of elliptical cross section for different values of the external field change $\Delta H_e/H_p(0)$ along the major axis.

Coupling Losses

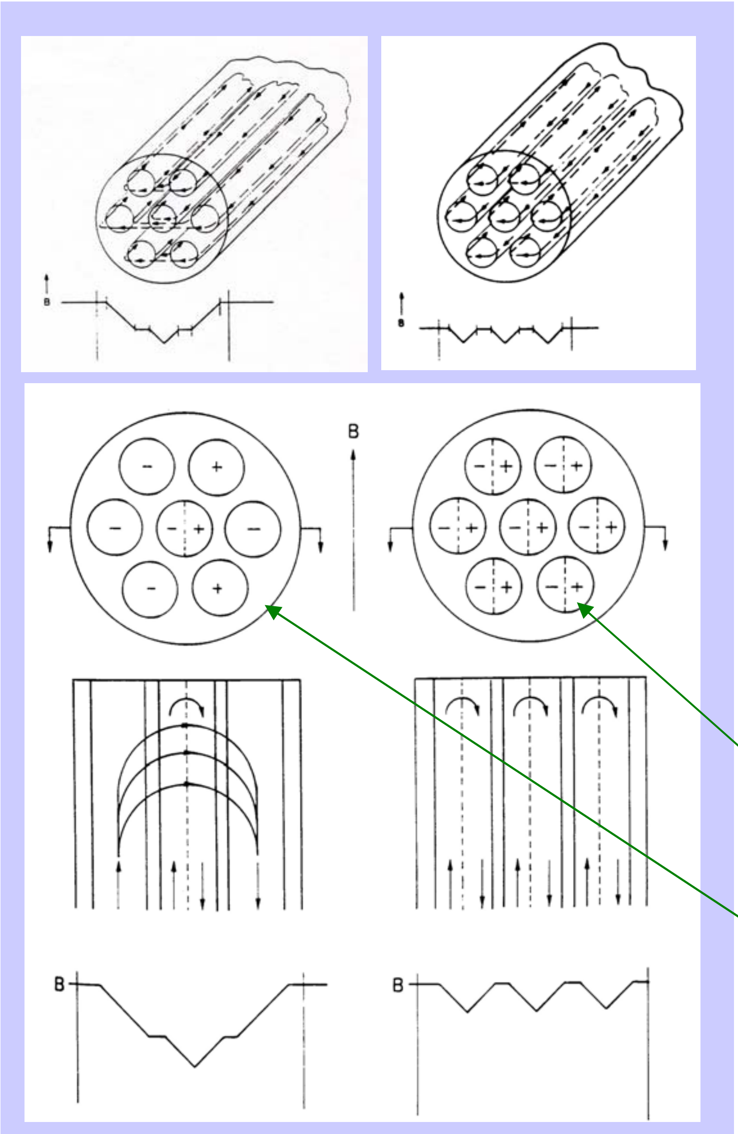

Twisting the superconducting filaments in the composite wire is necessary to electrodynamically decouple them

Hysteresis losses
$\propto$ filament diameter (~1 μm)

Hysteresis losses
$\propto$ strand diameter (~1 mm)

Coupling Losses

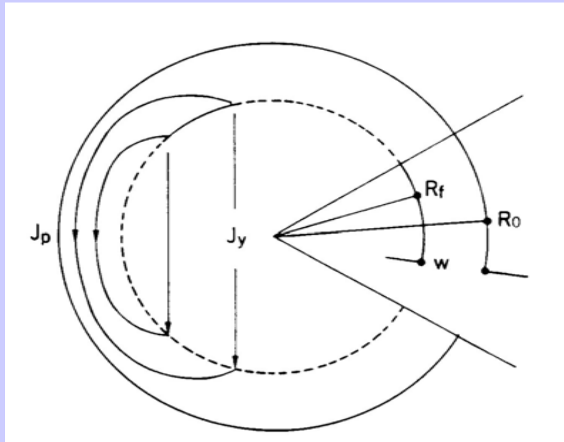

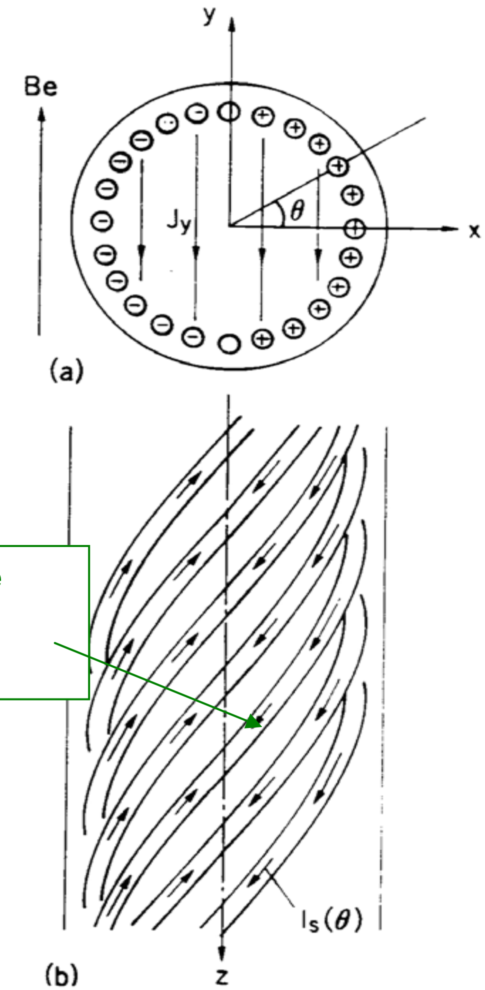

Twisting filaments also necessary to reduce coupling losses

Power dissipation ∝ (Twist Pitch)^2

Effective Matrix Resistivity

After W.J. Carr

$$\rho_{eff} = \frac{1-\lambda_f}{1+\lambda_f}\rho_m \qquad \textbf{Nb}_3\textbf{Sn}$$

$$\rho_{eff} = \frac{1+\lambda_f}{1-\lambda_f}\rho_m \qquad \textbf{NbTi}$$

λ_f = volume fraction of superconducting filaments
ρ_m = matrix resistivity [Ω-m]

Coupling Loss Power:

$$\frac{P}{Vol} = \frac{2\dot{B}^2}{\mu_o}\tau$$

AC Losses in Multistrand Cables

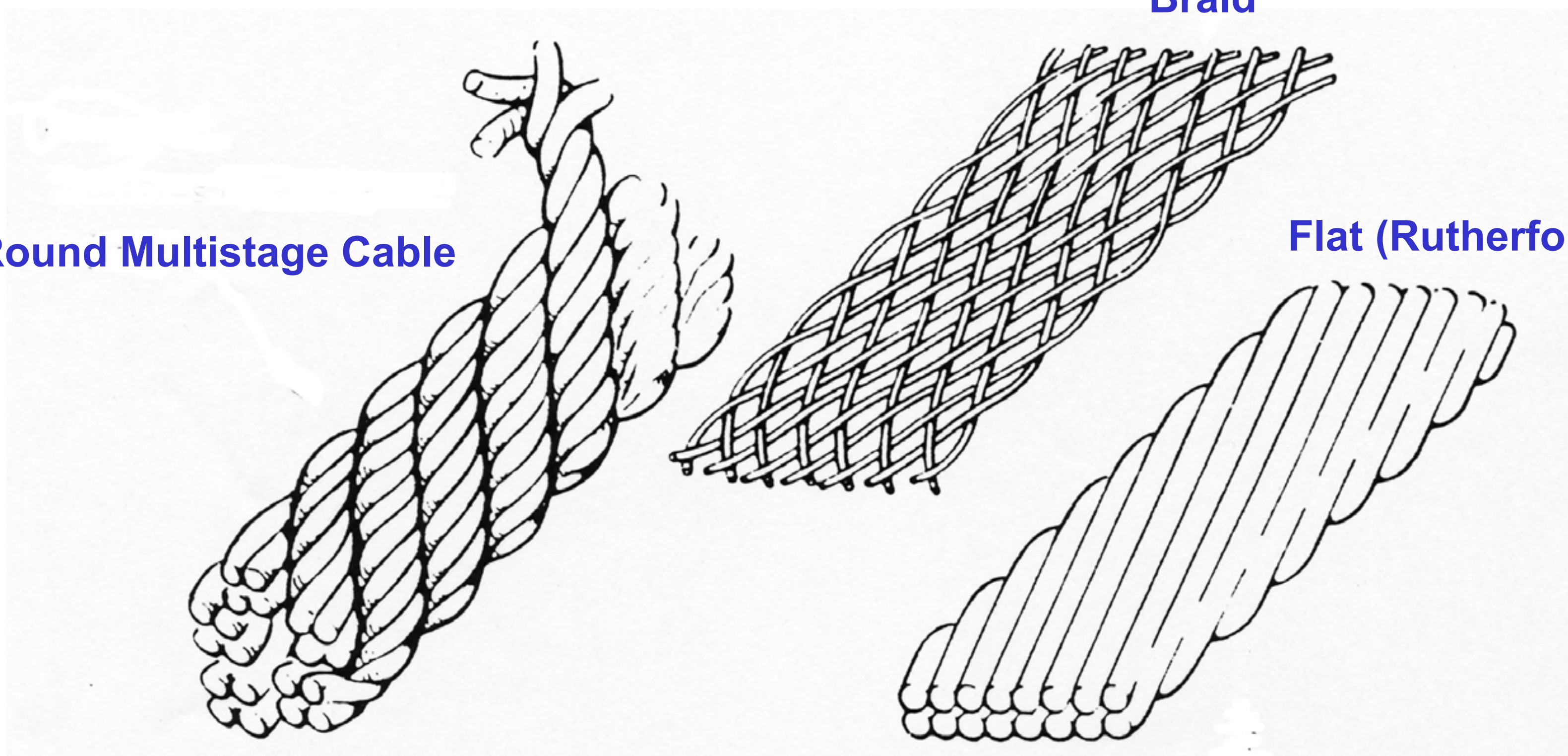

Reasons for Making Multistrand Cables:

- Increase current capacity
- Reduce AC and transient coupling losses
- Mechanical rigidity

AC Losses in Cables

Electromagnetic Analysis of AC Losses in Large Superconducting Cables

General Loss Components::

- **Hysteresis (magnetization) in superconducting filaments**
- **Coupling (intrastrand)**
- **Eddy (stabilizer)**
- **Coupling (inerstrand in sub-cables and cable-cable in built-up conductors)**

AC Losses

Electromagnetic Analysis of AC Losses in Large Superconducting Cables

Code output is calibrated against specific, well-controlled small scale laboratory experiments:

- **Useful for code calibration with limited boundary conditions**
- **Does not capture all full-size magnet operating conditions**

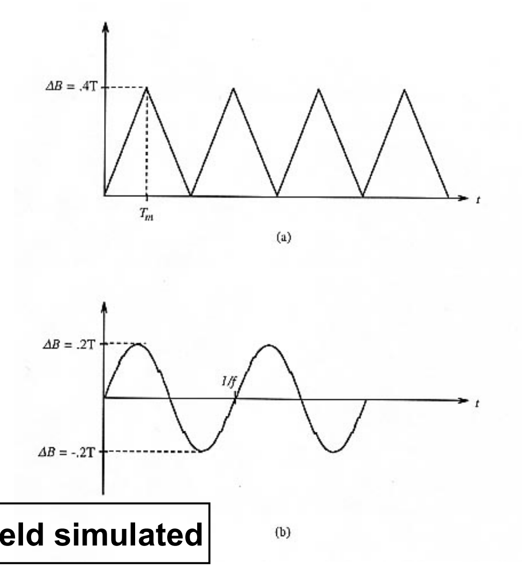

Linear ramp and sinusoidal AC field simulated

AC Losses

Electromagnetic Analysis of AC Losses in Large Superconducting Cables

Modeling a >1000 superconducting strand 5 stage cable

Individual strand locations in a 1/6th petal

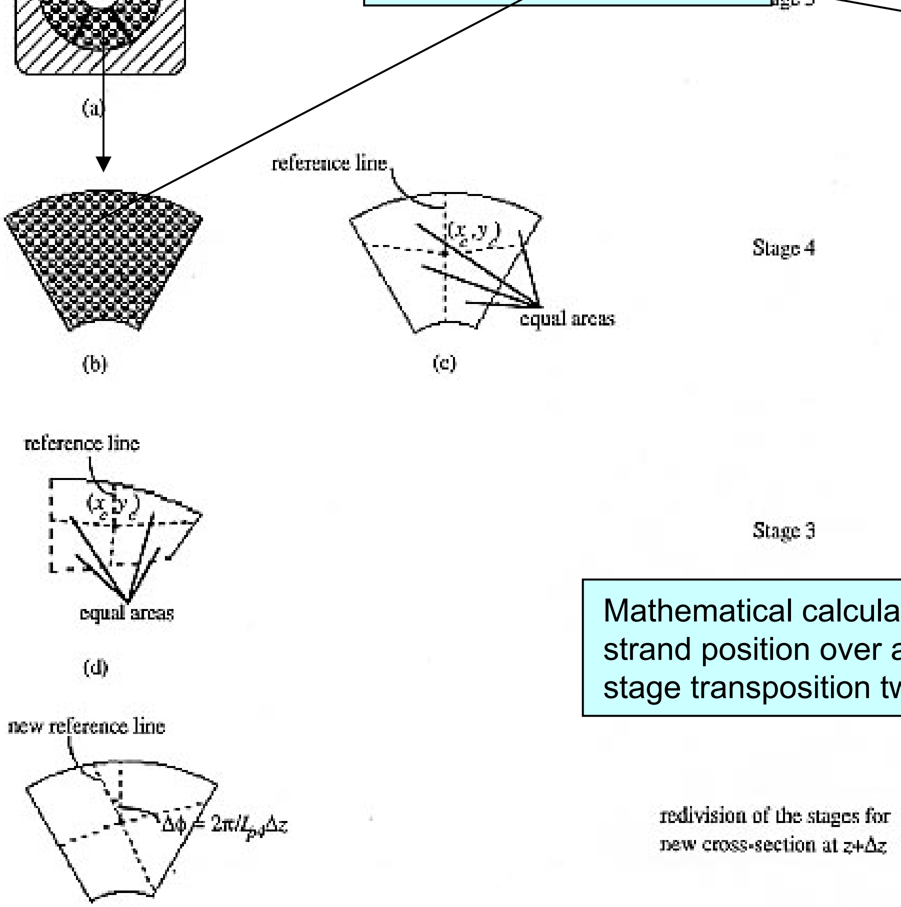

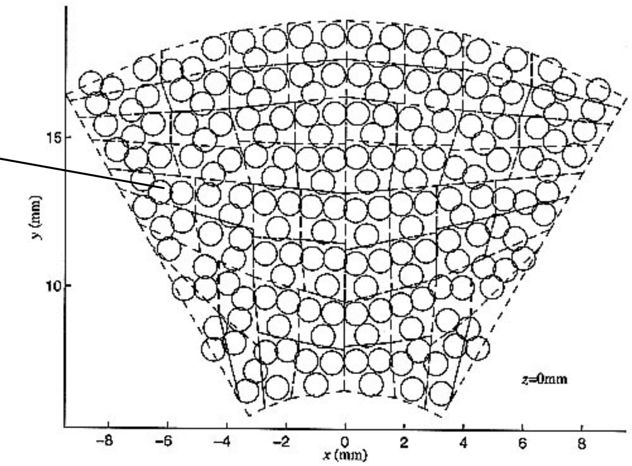

Mathematical calculation of strand position over a last-stage transposition twist pitch

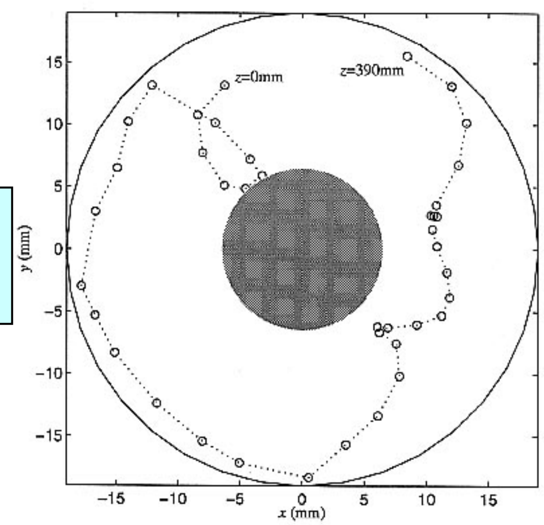

AC Losses- General Solution

For an infinitely long helically twisted strand or cable, the physical parameters $\dot{\rho} = 0$ and $\frac{\partial}{\partial z} = 0$. The governing equations (2.21) and (2.22) then reduce to

$$\nabla_T^2 \left(E_{\|} + \frac{\rho\dot{\psi}(r,\phi)}{r} \frac{\partial}{\partial \phi} \Phi \right) = \mu_0 \frac{\partial}{\partial t} \sigma_{\|} E_{\|} \tag{4.1}$$

$$\sigma_{\perp} \nabla_T^2 \Phi = \frac{1}{r} \frac{\partial}{\partial \phi} \left(\rho\dot{\psi}(r,\phi) \sigma_{\|} E_{\|} \right) \tag{4.2}$$

Expanding both equations and substituting the second into the first, we obtain

$$\nabla_T^2 E_{\|} + \frac{\rho\dot{\psi}}{r} \left[\frac{\rho\dot{\psi}}{r} \frac{\partial^2}{\partial \phi^2} + 2\left(\frac{\partial}{\partial \phi} \frac{\rho\dot{\psi}}{r}\right) \frac{\partial}{\partial \phi} + \left(\frac{\partial^2}{\partial \phi^2} \frac{\rho\dot{\psi}}{r}\right) \right] \frac{\sigma_{\|}}{\sigma_{\perp}} E_{\|}$$

$$+ \left[\nabla_T^2\left(\frac{\rho\dot{\psi}}{r}\right) + 2\left(\frac{\partial}{\partial r}\left(\frac{\rho\dot{\psi}}{r}\right)\frac{\partial}{\partial r} + \frac{1}{r^2}\left(\frac{\partial}{\partial \phi}\frac{\rho\dot{\psi}}{r}\right)\frac{\partial}{\partial \phi}\right) \right] \frac{\partial}{\partial \phi} \Phi = \mu_0 \frac{\partial}{\partial t} \sigma_{\|} E_{\|} \tag{4.3}$$

$$\nabla_T^2 \Phi = \frac{1}{\sigma_{\perp}} \left[\frac{1}{r} \left(\frac{\partial}{\partial \phi} \frac{\rho\dot{\psi}}{r} \right) \sigma_{\|} E_{\|} + \frac{\rho\dot{\psi}}{r} \frac{\partial}{\partial \phi} (\sigma_{\|} E_{\|}) \right] \tag{4.4}$$

With a single helicity cable or a multifilamentary strand, the filaments are twisted with one twist pitch of length L_p. This yields $\rho\dot{\psi} = \frac{2\pi}{L_p} r$ which reduces the equations even further to

$$\nabla_T^2 E_{\|} + \left(\frac{2\pi}{L_p} \right)^2 \frac{\partial^2}{\partial \phi^2} (\sigma_{\|} E_{\|}) = \mu_0 \frac{\partial}{\partial t} (\sigma_{\|} E_{\|}) \tag{4.5}$$

$$\nabla_T^2 \Phi = \frac{1}{\sigma_{\perp}} \frac{2\pi}{L_p} \frac{\partial}{\partial \phi} (\sigma_{\|} E_{\|}) \tag{4.6}$$

CSMC Measured Results

Typical distribution of coupling loss tau
for 18 layers x 2-in-hand =36 conductors

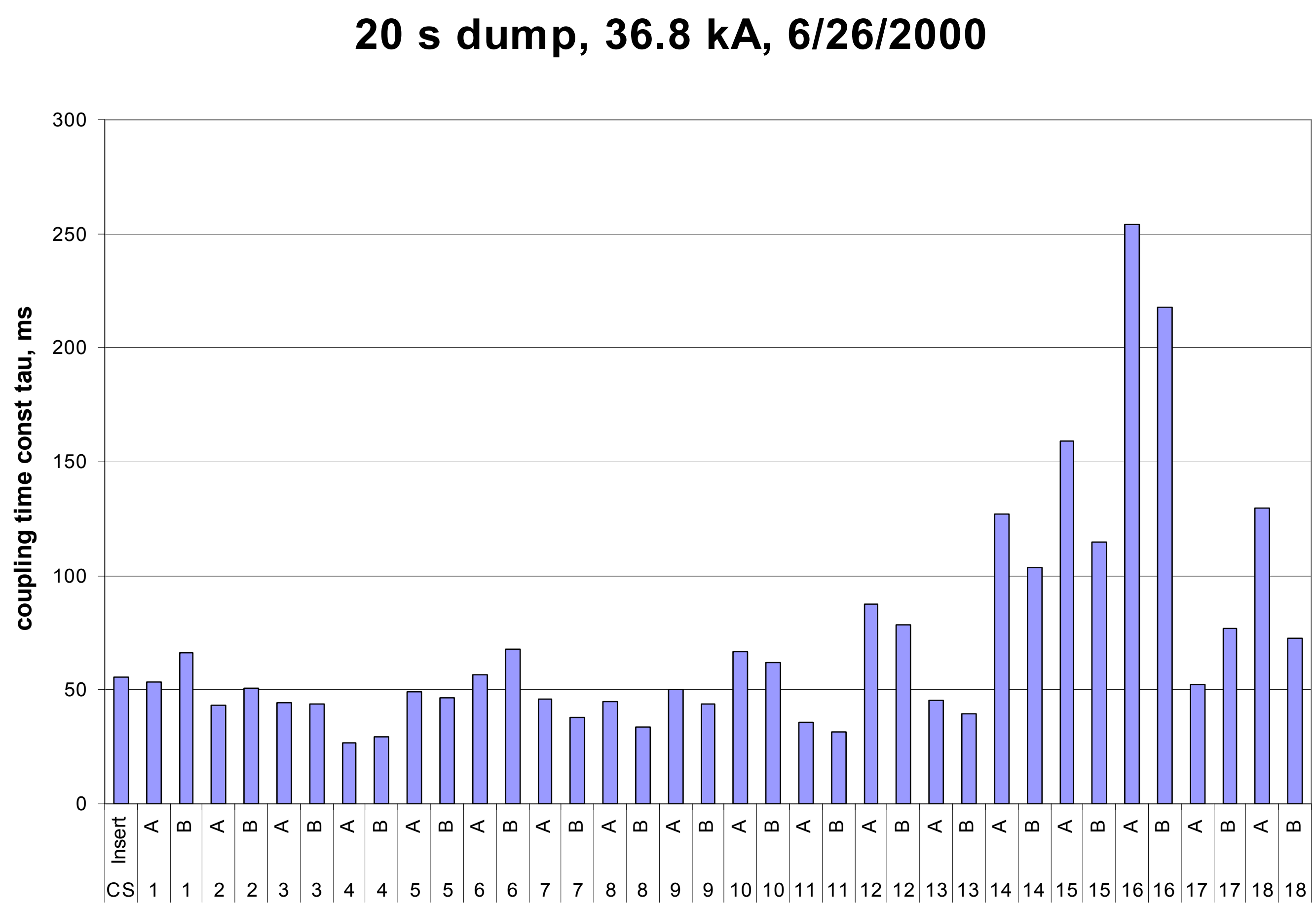

Effective cable coupling time constants vary greatly depending on cable twist pitches, magnitude of Lorentz Force (J x B), surface coating, magnetoresistance, and field magnitude.

CSMC Measured Results

Reduction of AC coupling losses with cycles

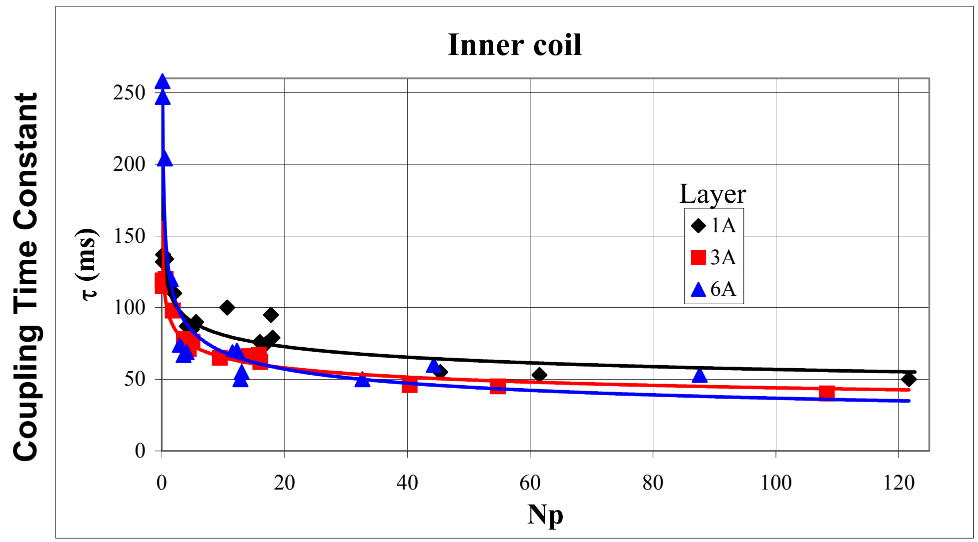

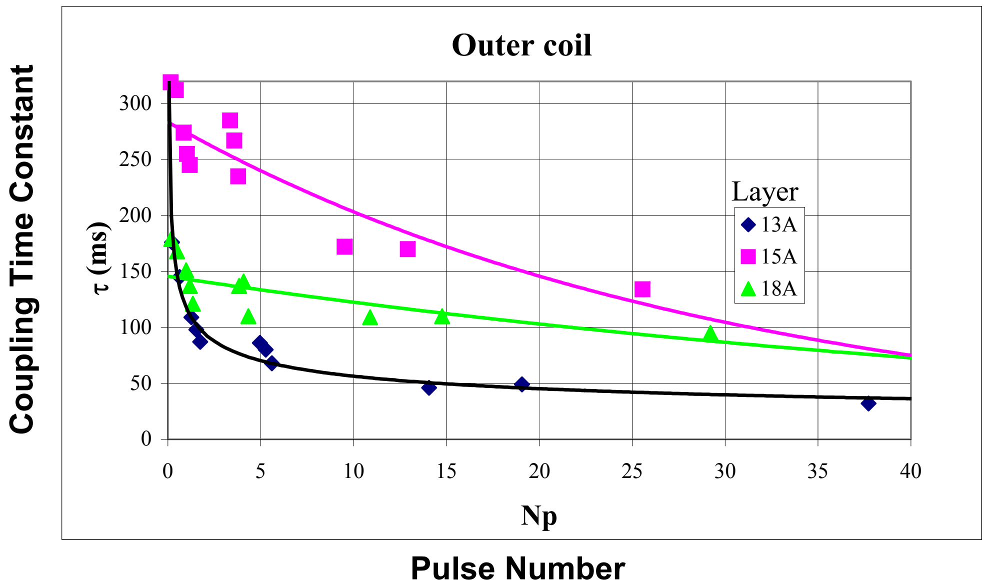

Thesis: **Cycling affects effective coupling time constant by changes in strand contact pressure distribution and interfacial resistance.**

- **An important (and often unknown a priori) parameter is the effective transverse conductivity between and among the wires and cable stages.**

- **A separate lab-scale experimental program is used to determine this parameter.**

Splice (Joint) Losses

Joule Dissipation, G_{sl}

$$G_{sl} = R_{sl} I_t^2$$

I_t = Transport current through the joint [A]
R_{sl} = Joint Resistance [Ω]

$$R_{sl} = \frac{R_{ct}}{A_{ct}} = \frac{R_{ct}}{a l_{sl}}$$

R_{ct} = contact resistance [Ω-m^2]
a = conductor width (joint width) [m]
l_{sl} = splice length [m]

Splice (Joint) Losses

- Surfaces can be in contact under pressure with no solder
  - then contact resistance depends on the surface condition. (roughness, surface oxides, etc.)
  - often silver plate.

- Surfaces are often soldered together
  - Some mechanical integrity- but often not too strong.
  - R_{ct} is usually > $\rho_{solder}\ \delta_{solder}$ because of contact resistance at solder-copper interface.
  - Best to measure

- Don't overheat joint during soldering because excessive temperature can reduce J_c of NbTi.

Joint Orientation to Field

2.2 Operation in varying field

coupling currents between strands and eddy currents in the copper soles are induced in the joint

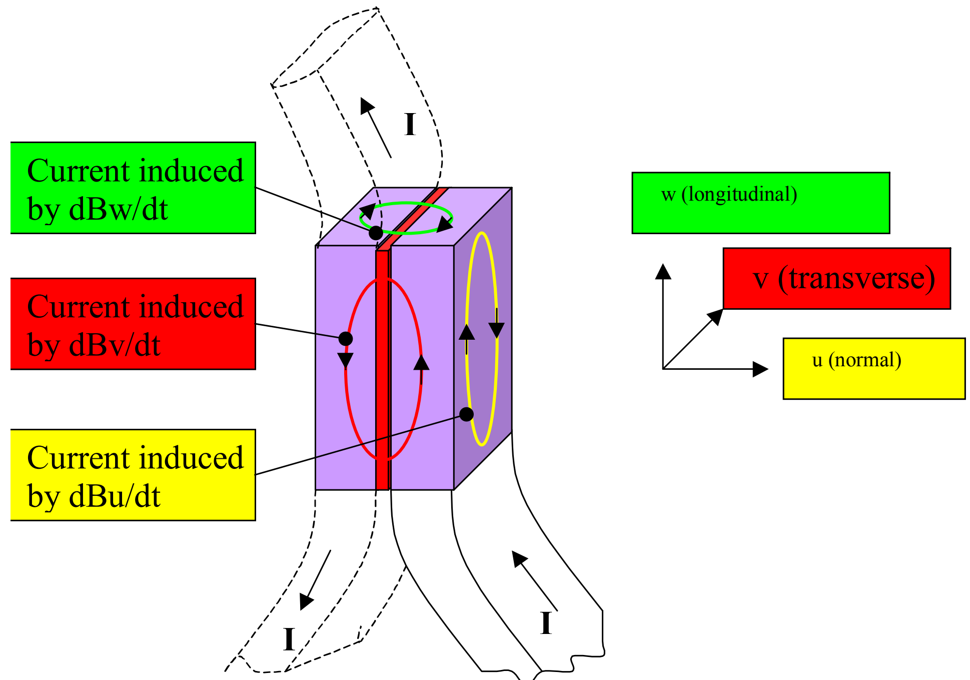

- transverse field variation (dBv/dt)

⇒ high intercable losses
⇒ low eddy current losses
⇒ risk of current saturation / flux jump
| ⇒ worst orientation

- normal field variation (dBu/dt)

⇒ interstrand losses
⇒ high eddy current losses (high RRR)
| ⇒ controlled losses

- longitudinal field variation (dBw/dt)

⇒ low interstrand losses
⇒ low eddy current losses
| ⇒ best orientation

US CSMC Joint Sample

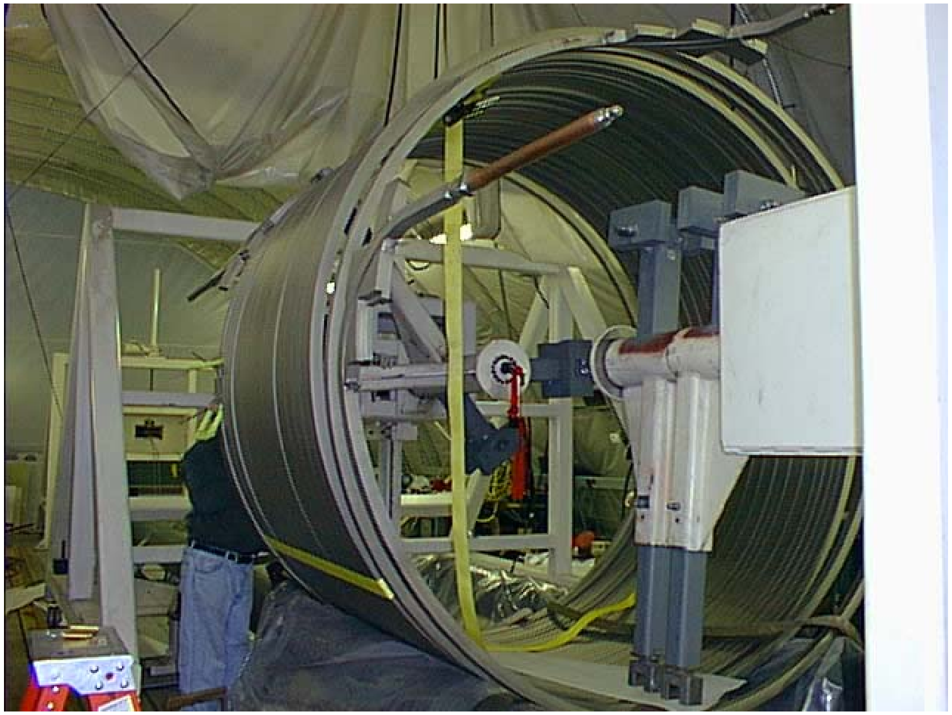

PTF Cryostat Sample Plumbing

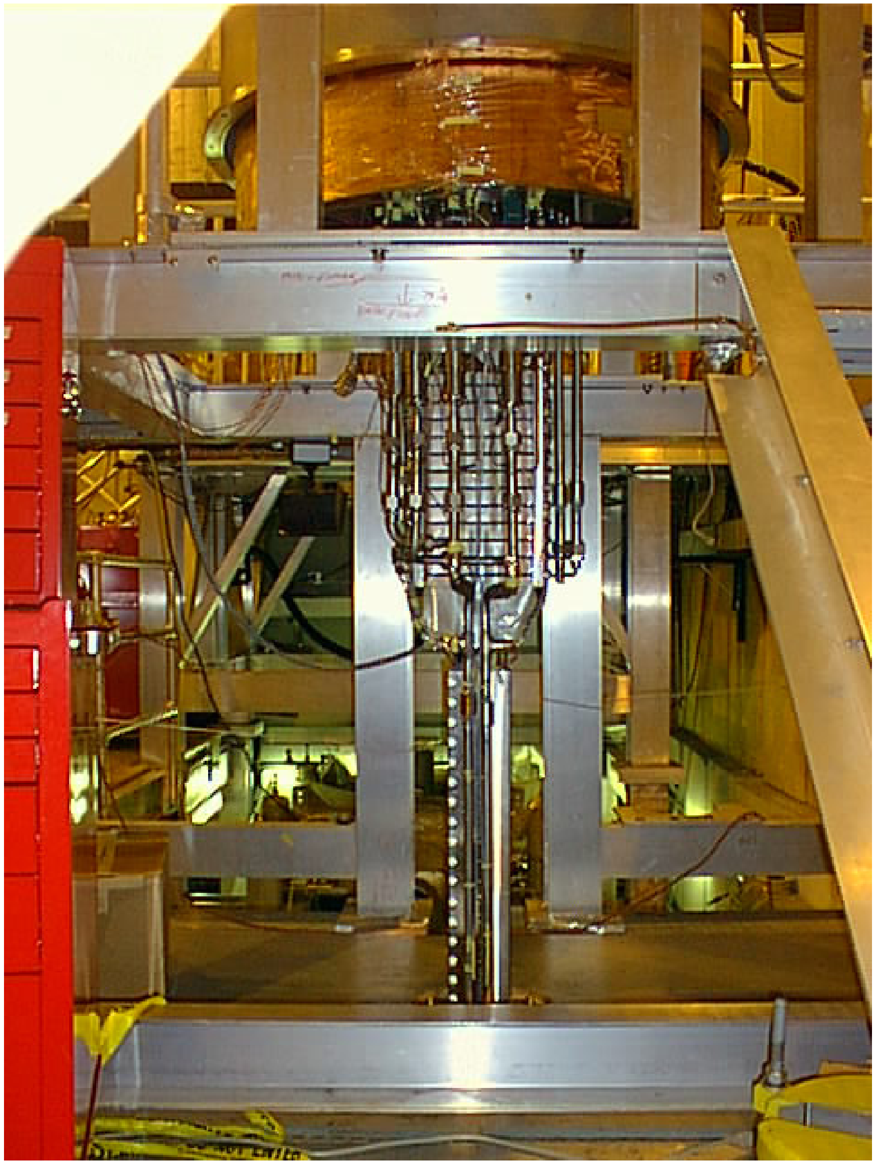

JA CSMC Butt Joint

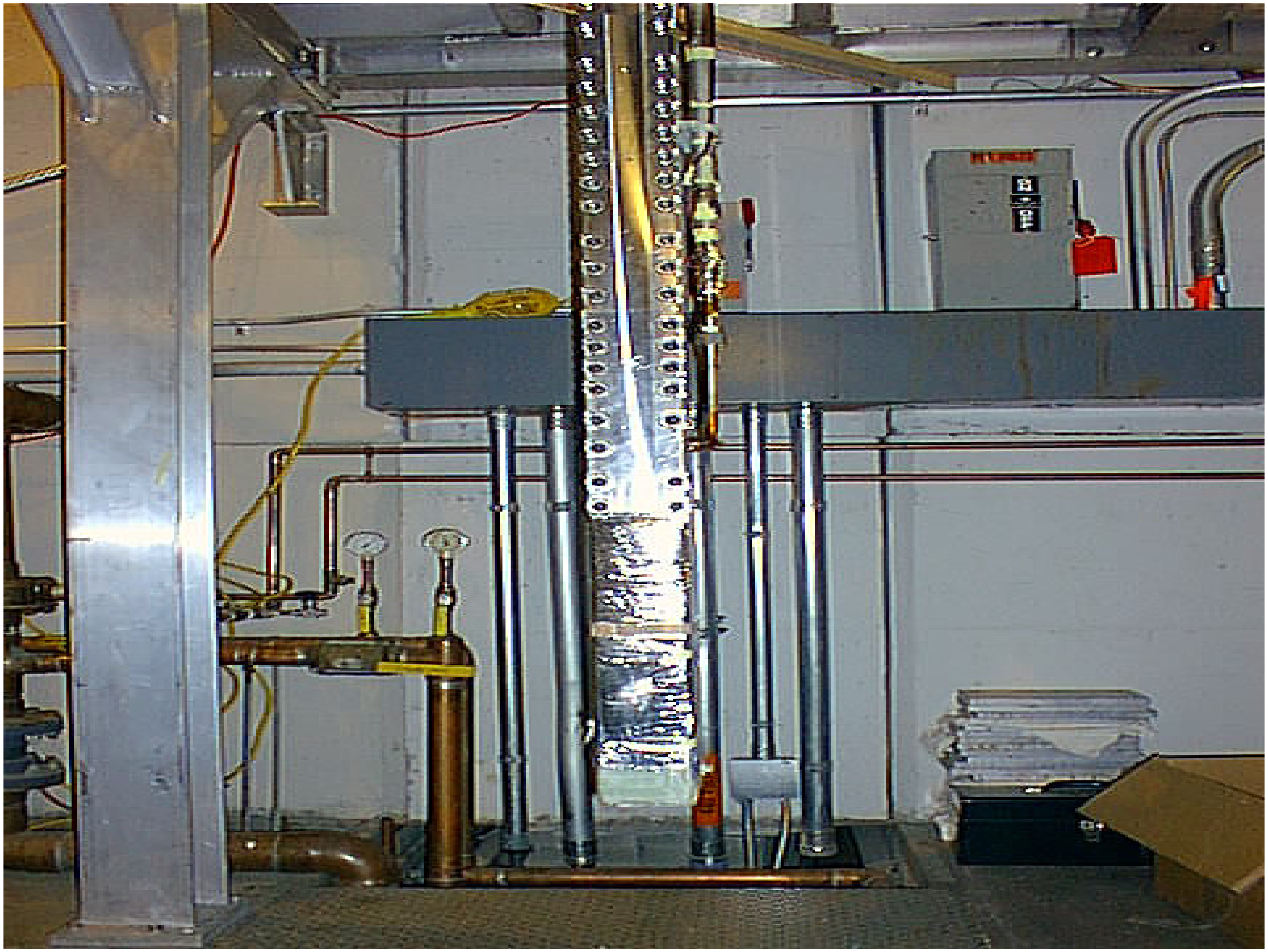

JA CSMC Butt Joint